ISSN 2354-9114 (online), ISSN 0024-9521 (print)
Indonesian Journal of Geography Vol 57, No.2 (2025): 312-333
DOI: 10.22146/ijg.102013 website: https://jurnal.ugm.ac.id/ijg

INDONESIAN JOURNAL OF GEOGRAPHY

RESEARCH ARTICLE

Spatio-temporal variability of Temperature and rainfall in the Jabitehinan District in North West Ethiopia

Addisu Bitew Birhanie[1, 2*], Daniel Ayalew Mengistu[1, 3]
[1]Department of Geography and Environmental Studies, Bahir Dar University, P.O. Box 79, Bahir Dar, Ethiopia
[2]Department of Geography and Environmental Studies, Debre Markos University, P.O. Box 269, Debre Markos, Ethiopia
[3]Geospatial Data and Technology Centre, Bahir Dar University, P.O. Box 79, Bahir Dar, Ethiopia

Received: 2024-11-29
Revised: 2025-04-04
Accepted: 2025-05-31
Published: 2025-07-31

Keywords: Invers Distance Weighted; climatic change; agro-ecological zones; and spatial variability.

Correspondent email:
addisubitew21@gmail.com

Abstract. Climate change, driven largely by human activities, leads to long-term shifts in temperature and precipitation. This study aimed to examine trends and spatiotemporal variability in rainfall and temperature in the Jabitehinan District, northwest Ethiopia, and assess their implications for agriculture and resource management. Historical climate data from the six meteorological stations in Ethiopian National Meteorological Agency were analyzed using Sen's slope estimator, the Mann-Kendall test, and the Precipitation Concentration Index, while spatial variability was assessed using the Inverse Distance Weighted method. Results revealed that mean seasonal rainfall reduction trends were 0.014 mm (spring), 0.005 mm (summer), 0.207 mm (autumn), and 0.057 mm (winter), with an annual average of 0.0122 mm. Temperature trends showed consistent increases: mean seasonal values rose by 0.189°C (winter), 0.215°C (spring), 0.184°C (summer), and 0.042°C (autumn), with an annual average rise of 0.206°C. Decadal trends showed increases in maximum, minimum, and mean temperatures at rates of 0.014°C, 0.029°C, and 0.037°C, respectively. The spatial distribution of rainfall was highest in the upper highlands (1790–1890 mm/year). About 57% of the middle district received 1768–1790 mm, while 20% of the area had 1790–1812 mm, 13% had 1746–1768 mm, and 10% received 1702–1746 mm annually. These findings highlight the substantial impact of climate variability on agricultural productivity, especially for rain-fed farming. They emphasize the need for climate-smart agricultural practices and inform policies aimed at supporting smallholder farmers in similar agro-ecological zones.

1. Introduction

Since rain-fed agriculture is the primary method of food production in the Horn of Africa—where Ethiopia is located—the region is particularly vulnerable to climate variability. Studies by Blein *et al.* (2017) and Khatri and Pasa (2023) highlight that rising temperatures and inconsistent precipitation are expected to reduce crop yields and overall agricultural productivity. Ethiopia features a wide range of agroclimatic zones, with rainfall and temperature distributions varying from semi-arid to humid and warm conditions (Regassa *et al.*, 2010). The mean annual rainfall also shows significant variation: while the southwestern highlands receive over 2,000 mm, the southeastern and northwestern plains get less than 300 mm (Yekoy, 2022). Similarly, the annual mean temperature varies greatly, ranging from over 25°C in the lowlands to below 15°C in the highlands (Degefu & Bewket, 2014). Ethiopia exhibits diverse agroclimates, with mean annual rainfall ranging from over 2,000 mm in the southwestern highlands to less than 300 mm in the southeastern and northwestern plains, and highly variable temperatures from semi-arid to humid and warm conditions (Regassa *et al.*, 2010). According to (Regassa *et al.*, 2010); Kew *et al.* (2017), it is over 25^{0}C in the lowlands and less than 15^{0}C in the highlands.

Ethiopia experiences four main seasons locally known as winter, spring, summer, and autumn. The dry winter season typically spans from December to February. The major rainy season locally called Kiremt occurs from June to August, while the shorter rainy seasons in spring and autumn occur from March to May and from September to November, respectively (Gissila *et al.*, 2004; Riddle & Cook, 2008; Regassa *et al.*, 2010; Kew *et al.*, 2017). However, there is significant variability in seasonal rainfall distribution across the country (Riddle & Cook, 2008; Kew *et al.*, 2017). The timing and intensity of the two rainy seasons—Kiremt (summer) and Belg (spring/autumn) directly affect agricultural productivity (Y. A. Tessema *et al.*, 2013; Teyso *et al.*, 2016; I. Tessema & Simane, 2019). Rain-fed agricultural activities are closely linked to rainfall patterns, delays in the onset of rain or early cessation are major contributors to crop failure (I. Tessema & Simane, 2019).

In the northern and eastern regions of Ethiopia, insufficient rainfall poses a similar threat, contributing to decreased crop and livestock productivity and exposing farm households to persistent food insecurity (Dinku, 2010; Asfaw *et al.*, 2018). Rainfall variability is cited as a key factor contributing to poverty, with approximately 30% of the Ethiopian population living below the poverty line (Regassa *et al.*, 2010; Ndaruzaniye & security, 2011). These challenges are especially acute in the area under study, where erratic temperature and precipitation patterns frequently lead to agricultural failure. Smallholder farmers are particularly vulnerable, as fluctuations in temperature and rainfall often result in crop loss and livestock mortality (NMSA, 2007). The impacts of climate variability and extremes in Ethiopia are among the most widely documented in both media and scientific literature (Gautam *et al.*, 2009).

Given this context, a comprehensive and detailed study is essential to understand trends in key meteorological variables at a fine spatial scale. Such analysis supports informed decision-making in sensitive sectors such as agriculture (Esayas *et al.*, 2019). Research indicates that examining the spatial and temporal characteristics of rainfall and temperature is critical for urban and agricultural planning (Mehmet, 2015), flood risk analysis, water resource assessments, and evaluating the impacts of climate change (Alemu, 2019). This study focuses on the northwest highland region of Ethiopia, where diverse topography results in marked spatial variability and distinct climatic patterns. These differences are evident in both seasonal and annual rainfall and temperature averages (Ademe *et al.*, 2020). The observed variability across seasons has significantly influenced the performance of agriculture, the region's dominant economic sector (Esayas *et al.*, 2019).

Rainfall and temperature variability and trends were documented by many scholars in Ethiopia (Woldeamlak Bewket & Conway, 2007; Abtew *et al.*, 2009; Bewket, 2009; Ayalew *et al.*, 2012; Jain & Kumar, 2012; Ahmed *et al.*, 2014; IPCC, 2014; Asfaw *et al.*, 2018; Abegaz & Mekoya, 2020; Ademe *et al.*, 2020; Alemayehu *et al.*, 2020b; Mekonen *et al.*, 2020; A. Alemayehu *et al.*, 2022; Wassie *et al.*, 2022; Yekoy, 2022). These studies were shown inconsistent results of seasonal and annual climate variability and trends mainly on rainfall variability and trend. The inconsistency might have originated from differences in spatial extent, study periods and geographic location. This study also believed that these differences might originate from the mountainous nature of the country that needs to investigate at local and/or micro-levels. In this regard, reports and scientific works such as (IPCC, 2000; Easterling *et al.*, 2007; Bewket, 2009) evidently pointed out that local scale spatiotemporal rainfall and temperature variability and trends in many parts of Ethiopia remain unknown and needs scientific investigation at the local level. More specifically, Gissila *et al.* (2004) noted that though analyses of spatiotemporal rainfall and temperature variability and trends at national and regional levels are imperative, analysis at the local level is equally important for water management, food security analysis, and disaster risk management. This study has two research questions: 1) what are the trends in rainfall and temperature (maximum, minimum, and mean) across different seasons (spring, summer, autumn, and winter) and on an annual basis in the Jabitehinan District? 2) How does the spatial variability of rainfall and temperature manifest across different areas of the Jabitehinan District, as determined using the Inverse Distance Weighted (IDW) spatial analysis method? The authors contribute empirical evidence, methodological rigor, and practical recommendations that together support climate resilience in agriculture and resource management.

An international reader of the journal can gain several important insights from this study on the spatiotemporal variability of temperature and rainfall in the Jabitehinan District, northwest Ethiopia: Broader Understanding of Climate Change Impacts in Vulnerable Regions: the study offers a clear example of how climate change is manifesting at a local scale in sub-Saharan Africa. It adds to the global discourse by providing empirical data from a region where agriculture is highly sensitive to climate variability, but where such detailed analyses are often underrepresented in the literature. Methodological Application in Data-Scarce Settings: by using robust statistical tools like Sen's slope estimator, the Mann-Kendall test, and the Inverse Distance Weighted (IDW) method, the paper demonstrates how meaningful climate trend analyses can be conducted even in regions with limited meteorological infrastructure, offering a replicable model for similar regions globally. Insight into Rainfall and Temperature Trends over Time: international readers can observe long-term, seasonal, and decadal changes in rainfall and temperature in a semi-arid region. These changes are quantified, showing trends such as temperature increases and rainfall reduction, which are critical indicators of climate risk. Agricultural and Policy Implications: the paper underscores the direct link between climate trends and agricultural productivity, especially for rain-fed farming systems, which are prevalent in many developing regions. The findings inform climate-smart agricultural strategies and adaptation planning, relevant to policymakers, development agencies, and climate resilience practitioners worldwide. Relevance to Similar Agro-Ecological Zones Globally: the study's conclusions are not only relevant to Ethiopia but also to other regions with similar topographic and climatic conditions. It contributes comparative data that can aid in regional and global climate resilience strategies.

While many studies examine global or national climate trends, this research provides a detailed, district-level analysis of long-term temperature and rainfall patterns. Such localized studies are relatively rare but crucial for effective climate adaptation. The study combines Sen's slope estimator, the Mann-Kendall test, the Precipitation Concentration Index (PCI), and Inverse Distance Weighted (IDW) spatial interpolation. This integrated approach strengthens the reliability of the analysis and adds depth to the understanding of both temporal and spatial variability. Unlike most climate studies that focus solely on temporal changes, this research maps the spatial distribution of rainfall and temperature across different zones within the district. This spatial perspective adds a new layer of insight, highlighting climate disparities within relatively small geographic areas. The study goes beyond reporting trends by explicitly linking climate variability to agricultural productivity and resource management. It stresses the need for climate-smart practices, which offers a practical direction for future adaptation measures and policy decisions.

Therefore, this study aims to examine the trends and variability of seasonal and annual rainfall and temperature in the district, as well as to illustrate their spatial distribution and variation. The findings will offer valuable insights for informed decision-making and strategic planning, supporting the implementation of effective measures to reduce the impacts of climate variability on the environment. This is vital for promoting sustainable economic development, particularly in climate-sensitive sectors like agriculture.

2. Methods

Description of the study area

Jabitehnan district is found in the Amhara National regional state, at West Gojjam zone of Ethiopia. It is located on 10^0 30'0" N-10^0 50' 0" N and 37^0 4' 0" E-37^0 32' 0" E. The majority of the woreda lies in altitude from 1500-2300m. Agro-ecologically, 88% of the woreda is classified as subtropical and the remaining 12% as *kola (DistictAgricultureoffice, 2020)*. The temperature of the district ranges between 14^{o}_{c} to 32^{0}_{c}, with an annual average of 23^{0}_{c}. The average annual rainfall is 1250mm per annum (DistictAgricultureoffice, 2020). Small-scale mixed farming is the main economic activity in the rural community of the district, with crop production being the major economic activity followed by livestock production. The district is known as area of surplus production of all kind of farming production of all cereal and cash crop production. Livestock production is the second most important economic activity for the district a whole (DistictAgricultureoffice, 2020). Jabitehinan district is selected as the study area for the following reasons.

Jabitehinan stands out as one of the 15 districts within the West Gojjam administrative zone. Positioned 374 kilometers Northwest of Addis Ababa and 171.7 kilometers southwest of Bahir Dar, the Regional State capital, this district encompasses a total area of 117,020 hectares. Presently, it is organized into 37 rural sub-districts administrations and hosts 3 towns Finote Selam, Mankusa, and Jiga being the principal ones. According to UNDP (2007) report the "human population of Jabitehinan is 270,147; among them 253,348 reside in rural areas, while the remaining 16,799 inhabit urban areas".

Data Sources and Data Analysis

Gridded monthly precipitation data for the Greater Horn of Africa was sourced at a spatial resolution of 0.10° x 0.10°, offering a comprehensive and precise dataset. In contrast, temperature data with a resolution of 0.50° x 0.50° was obtained from the Climate Research Unit (CRU) Time-Series (TS) dataset. Additionally, the Ethiopian National Meteorological Agency (ENMA) – West Amhara Meteorological Service Centre in Bahir Dar provided long-term, station-based historical monthly meteorological data covering the period from 1981 to 2022.

To enhance the accuracy of the gridded datasets, statistical bias correction techniques such as quantile mapping were employed. These methods were used to adjust the gridded data to more closely align with the station-based observations.

The study utilized data from six meteorological gauge stations characterized by high data quality, long-term records, and good spatial distribution across the region. As discussed in the following sections, various statistical indicators and tests were applied to analyze the spatiotemporal variability and trends in rainfall and temperature. In particular, the coefficient of variation (CV) and the Precipitation Concentration Index (PCI) were used to assess the temporal variability of rainfall.

The temporal variability of rainfall was displayed using the coefficient of variation.

Where: mean, standard deviation, and coefficient of variation (CV, σ). Therefore, a coefficient of variation of less than 20 indicates reduced variability, a coefficient of variation between 20% and 30% indicates moderate variability, and a coefficient of variation larger than 30% indicates significant rainfall variability (Alemayehu *et al.*, 2020a). The concentration of yearly and seasonal rainfall was shown using the Precipitation Concentration Index (PCI).

$$PCI_{annual} = \frac{\sum_{1}^{12} = 1pi2}{(\sum_{1=1}^{12} pi)\ 2} \text{ (x 100)} \quad ....(1)$$

$$PCI_{Seasonal=} \frac{\sum_{1=1}^{4} {}_{pi}^{2}}{(\sum_{1=1}^{4} pi)\ 2} \text{ (x 33.3)} \quad ....(2)$$

Where: *pi* is the monthly rainfall in i^{th}

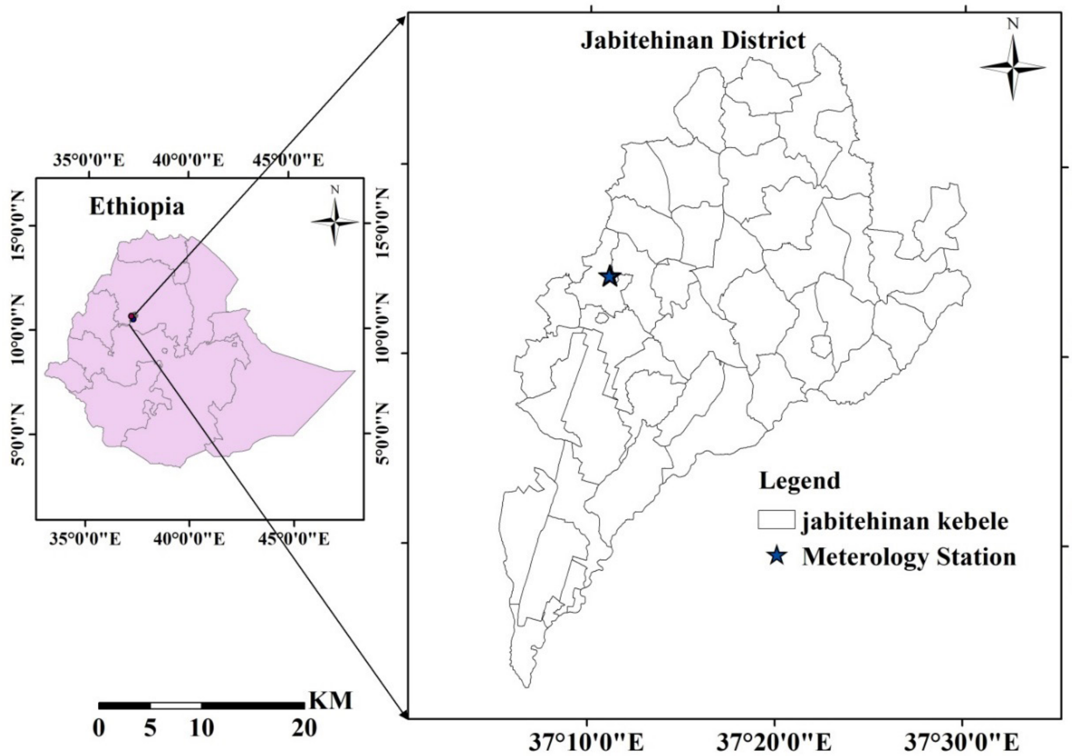

Figure 1. Study Area Map

Sen's Slope Estimator and the Mann-Kendall (MK) Test: Sen's Slope estimator and the non-parametric Mann-Kendall (MK) test were used to examine the patterns and amounts of temperature and precipitation. In particular, the annual and seasonal (belg and kiremt) rainfall and temperature data were evaluated using the MK trend test. The temperature and rainfall data, both yearly and seasonal (belg and kiremt), were analysed using the non-parametric MK trend test. In several climatological and hydrological time series applications, the MK test is frequently utilised as the most efficient technique for statistically significant trend test identification (NMSA, 2007; Ademe *et al.*, 2020; Alemayehu *et al.*, 2022). Additionally, the MK test is preferred over other tests since its procedures are less sensitive to outliers or robust against the influence of extremes (NMSA, 2007); can test trends in a time series without requiring normality or linearity, which is a distribution-free test (Alemayehu *et al.*, 2022). As a result, the World Meteorological Organisation strongly advises against using it generally (Alam *et al.*, 2017). The MK test is used to determine whether temperature variability and rainfall have a statistically significant or non-significant trend (Jain & Kumar, 2012). According to (Suryabhagavan, 2017), a positive value denotes an increasing trend while a negative value denotes a decreasing trend over time.

The selection of Sen's slope estimator and the Mann-Kendall test was driven by the specific goals of this study to analyze the trend and magnitude of changes over time in a reliable, robust, and non-parametric way. Both methods are widely used in environmental and climate studies, especially when dealing with time series data that may not follow a normal distribution or where data may exhibit outliers, skewness, or non-linearity.

Sen's Slope: This method was chosen to estimate the magnitude of the trend because it is a non-parametric approach that is less sensitive to outliers than traditional linear regression. It provides a robust estimation of the slope of the trend, especially useful for time series data with potential irregularities. Sen's slope is particularly appropriate when the data is noisy or non-linear, as it calculates the median of all possible pairwise slopes between data points, making it resistant to extreme values that could distort the results.

Mann-Kendall Test: The Mann-Kendall test was selected to assess the statistical significance of the trends detected by Sen's slope. It is a non-parametric test that evaluates whether there is a monotonic increasing or decreasing trend over time. This method is advantageous because it does not require the data to meet assumptions of normality and can handle both seasonal and non-seasonal data effectively. The test also provides a clear indication of whether trends are statistically significant, which is critical in understanding whether observed changes are likely due to real phenomena or simply random variation.

The following formulas were used to calculate the MK statistic S, its variance, and the related standard normal test statistic:

$$\sum_{i=1}^{N-1} \quad \sum_{j=i+1}^{N} sgn(xj - xi) \text{ .... (3)}$$

Where: N is the number of data points; X_i and X_j are the time series observations.

Assuming $(x_j - x_i) = \theta$, the value of sgn (θ) is computed from:

$$\text{Sgn } (\Theta) = \begin{cases} +1 \ldots\ldots \theta & > 0 \\ 0 \ldots \theta & = 0 \\ -1 \ldots\ldots \theta & < 0 \end{cases} \text{ .... (4)}$$

Under the hypothesis of independent and randomly distributed variables, for large samples ($n \geq 10$), the σ statistic is approximately normally distributed, with zero mean and variance as:

$$\sigma 2 = \frac{n(n-1)(2n+5)}{18} \text{ .... (5)}$$

Thus, the distribution of the standardized normal deviate (Z-statistics) will subsequently be computed as:

$$Z = \begin{cases} S - 1/\sigma & if\ S>0 \\ 0 & if\ S=0 \\ S + 1/\sigma & if\ S<0 \end{cases} \text{ .... (6)}$$

As previously mentioned rising trends are denoted by a positive Z value and falling trends by a negative Z value. Similarly, trend magnitude has been measured using Sen (1968) non-parametric slope estimator processes in order to assess the relative strength of the MK trend test in time series data. Sen's slope estimator is frequently employed to ascertain the trend magnitude in hydro-meteorological time series, as mentioned by (I. Tessema & Simane, 2019). Because of its comparatively low sensitivity to extreme values, it is a robust estimator (Chattopadhyay & Edwards, 2016). The slopes of each pair of data are calculated using (Chakraborty *et al.*, 2013) in order to provide an estimate of the slope bi, as follows:

$$\text{bi} = \frac{xj-xi}{j-i}, i = 1,2,3, \ldots N, j > i \text{ ....(7)}$$

Where: xj and xi are data values at times j and i. The Sen's estimator of the slope is the median N values of bi:

$$\text{b} = \begin{cases} b(N+1)/2 & if\ N\ is\ odd \\ 0.5[bN/2 + b(N+2)/2] & if\ N\ is\ even \end{cases} \text{ .... (8)}$$

A positive value of b indicates an increasing value with time while a negative of b indicates a decreasing value with time.

Inverse Distance Weighted (IDW): Although gridded data were used in this study, Inverse Distance Weighting (IDW) interpolation was employed to refine the spatial resolution and fill in gaps where data points were sparse or unevenly distributed. The original gridded dataset did not provide adequate spatial coverage at the scale required for our analysis, particularly in regions with complex topography or variable data density. IDW was chosen due to its simplicity, transparency, and effectiveness in scenarios where spatial autocorrelation is assumed — that is, where nearby points are more likely to have similar values.

The choice of IDW over other interpolation methods (e.g., kriging or spline) was based on its computational efficiency and ease of implementation, especially in large datasets. Furthermore, preliminary tests showed IDW performed comparably well in terms of accuracy for this dataset.

To validate the IDW interpolation, a cross-validation procedure was carried out using a subset of observed data. This involved removing a portion of known data points, performing the interpolation, and then comparing the interpolated values against the actual data. The resulting root mean square error (RMSE) and mean absolute error (MAE) were within acceptable limits, indicating that IDW provided a reasonable approximation for the spatial patterns present in the data (Ahrens & Sciences, 2006). For the purpose of identifying and calculating variability and trends (time series) of annual and seasonal rainfall and temperature values, the XLSTAT 2014 programme and Excel spread sheet were utilised. The trend's magnitude was also discovered using Sen's approach. Temperature and rainfall data were subjected to a geographical trend analysis using Geographic Information Systems (GIS version 10.1).

3. Results and Discussions

Temporal variability of rainfall

The study areas long-term mean annual rainfall, as indicated in Table 1, was 1000.9 mm, with an 87.2 standard deviation and an 8.7% coefficient of variation. With a standard deviation of 32.77 and a coefficient of variation of 3.28%, the decadal mean rainfall was 998.48 mm. The years with the lowest mean annual rainfall (674.1 mm) and the greatest (1251.9 mm) were 1916 and 1984, respectively. Spring produced 23% of the annual total rainfall, whilst summer contributed roughly 68.4%. In the Woleka sub-basin of South Wollo, Asfaw *et al.* (2018) reported a similar study showing that the summer and spring seasons provide 74.4% and 13% of the rainfall, respectively. Similarly, research in the Amhara Region (Ayalew *et al.*, 2012) and the Upper Blue Nile basin (Abtew *et al.*, 2009) found that the summer season accounts for the largest portion of the yearly rainfall total. Numerous more studies (UNFCCC, 2007; Asfaw *et al.*, 2018; Z. Y. Alemayehu *et al.*, 2022) showed that in many places of Ethiopia, the spring season contributes significantly less (5%–30%) to the total annual rainfall than the summer season (64%–85%).

The coefficient of variation (CV) can be used to evaluate the variability of rainfall. Rainfall variability is classified as low when CV is less than 20, moderate when CV is between 20 and 30, and high when CV is greater than 30 (Hare, 2003). The winter season (December, January, and February) had a substantially larger coefficient of variation (115.0604%) than the summer season (June, July, and August), which had a CV of 21.30%. Research conducted in Ethiopia's Amhara Region (Bewket, 2009; Ayalew *et al.*, 2012; Rosell, 2013) revealed comparable findings, namely that the winter season's CV was greater and more unpredictable than the summer season's. The Mann-Kendall (MK) test and Sen's slope were used to detect and quantify trends in seasonal and annual rainfall. There is a slight decreasing trend in winter rainfall, but it is not statistically significant. The variability is very high (CV = 115.06%), indicating inconsistent patterns across years. A statistically significant increasing trend in spring rainfall is observed. The positive Sen's slope indicates an average increase of 4 units per year, suggesting that spring rainfall is becoming more abundant. A significant decreasing trend is detected in summer rainfall. The negative Sen's slope shows a reduction of about 10 units per year, which may impact water availability during the hottest season. Autumn also shows a significant decreasing trend in rainfall, with a drop of around 9 units per year. This could have implications for post-monsoon agriculture or hydrology. Overall, annual rainfall is declining at a statistically significant rate, with an average decrease of 4 units per year. Table 2 illustrates that, for the years 1981 to 2022, the annual PCI was predominantly characterised by a high proportion of erratic rainfall distribution (55.4%) over the observed years. While the spring and autumn seasons exhibit high concentration/irregular rainfall distribution and very high concentration/irregular rainfall distribution (49.5%) and (42.3%) of the seasons, respectively, the summer season belongs to High concentration/irregular rainfall distribution (17.4%). Similar findings are reported by (Bewket, 2009; Ayalew *et al.*, 2012; Asfaw *et al.*, 2018), showing that the summer months have higher concentrations of rainfall.

Table 1. Rainfall trend analysis by seasonal, and MK test (1981-2022)

Variable	Minimum	Maximum	Mean	Std. deviation	CV (%)	MK Test	Sen's Slope
winter	0.000	51.267	9.991	11.496	115.060	-0.057	-2
Spring	22.853	198.633	84.797	37.314	44.003	0.111**	4
summer	181.057	478.127	338.166	72.047	21.305	-0.277**	-10
autumn	38.673	210.937	118.729	43.250	36.427	-0.253**	-9
Annual	901.760	2515.430	1655.051	382.931	23.137	-0.111**	-4

** is statistically significant when P is less than 0.05.
Source Ethiopian Meteorological Agency (2022)

Table 2. Precipitation Concentration Index (PCI) per season (winter, spring, summer, autumn, and annual) for 1981–2022

PCI Index (%)	Description	Observation seasons (%)				
		Winter	Spring	Summer	Autumn	Annual
<10	Uniform rainfall distribution/low concentration	-	-	-	-	-
10-15	Moderate rainfall distribution	-	-	-	-	-
16-20	High concentration/irregular rainfall distribution	-	49.5	17.4	-	55.1
>21	very high concentration/ irregular rainfall distribution	79.3	-	-	42.3	-

Trends of rainfall

With the exception of May and June, the Mann-Kendall test result showed a statistically significant declining trend in rainfall, as shown in Table 1. Additionally, the results showed that seasonal (winter, summer, and autumn) and annual rainfall displayed a significant decreasing trend, while spring season rainfall showed a non-significant decreasing trend (Wagesho *et al.*, 2013; Asfaw *et al.*, 2018; I. Tessema & Simane, 2019). However, a number of researchers indicate statistically non-significant trend results (Seleshi & Zanke, 2004; McSweeney *et al.*, 2008; Suryabhagavan, 2017). For winter, spring, summer, autumn, and annual rainfall, respectively, the regression coefficients also showed declining trends at the rates of 0.112mm/year, -0.229mm/year, -0.676mm/year, -0.844mm/year, and -10.912mm/year**Error! Reference source not found.**. Rainfall reduction exhibited variations among winter, spring, summer, autumn and yearly at a rate of 0.014mm, 0.005mm, 0.207m and m 0.057mm, and 0.0122 correspondingly. The decrease in yearly and summer rainfall, however, is not determined to be substantial. A similar outcome was found by (Jury & Funk, 2013) in the decrease of yearly rainfall at a rate of -0.4mm/year.

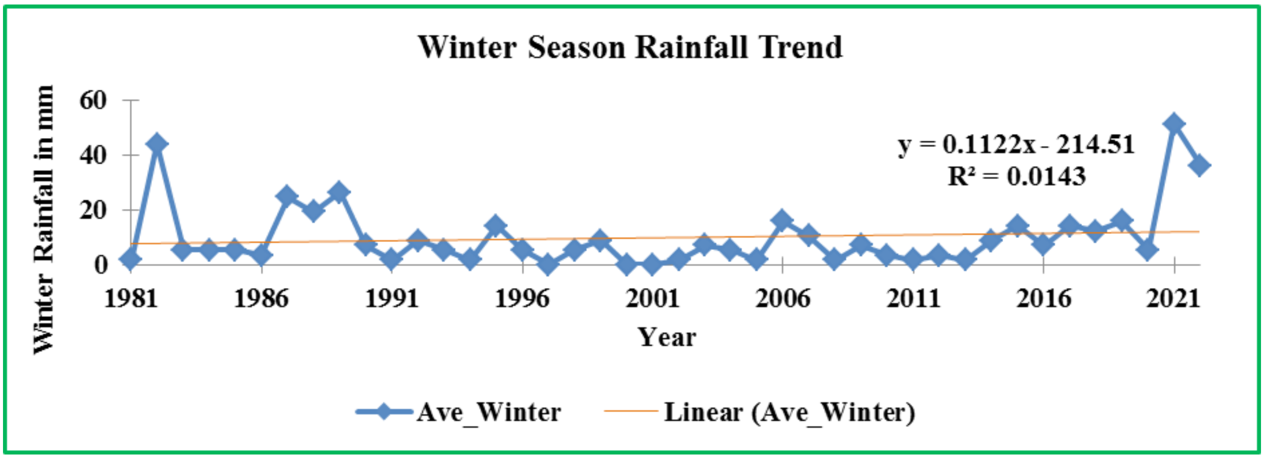

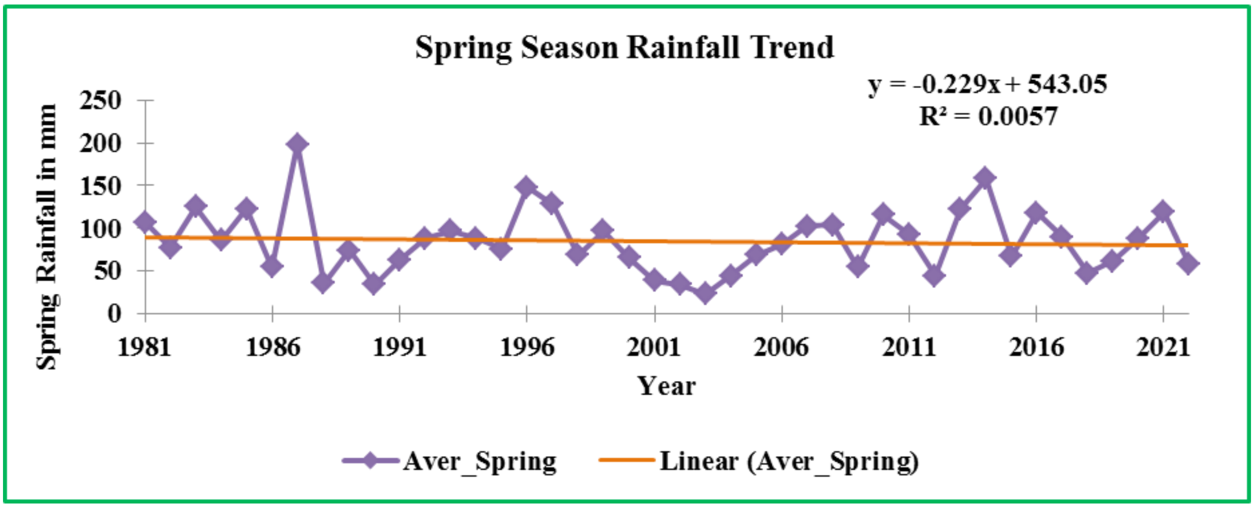

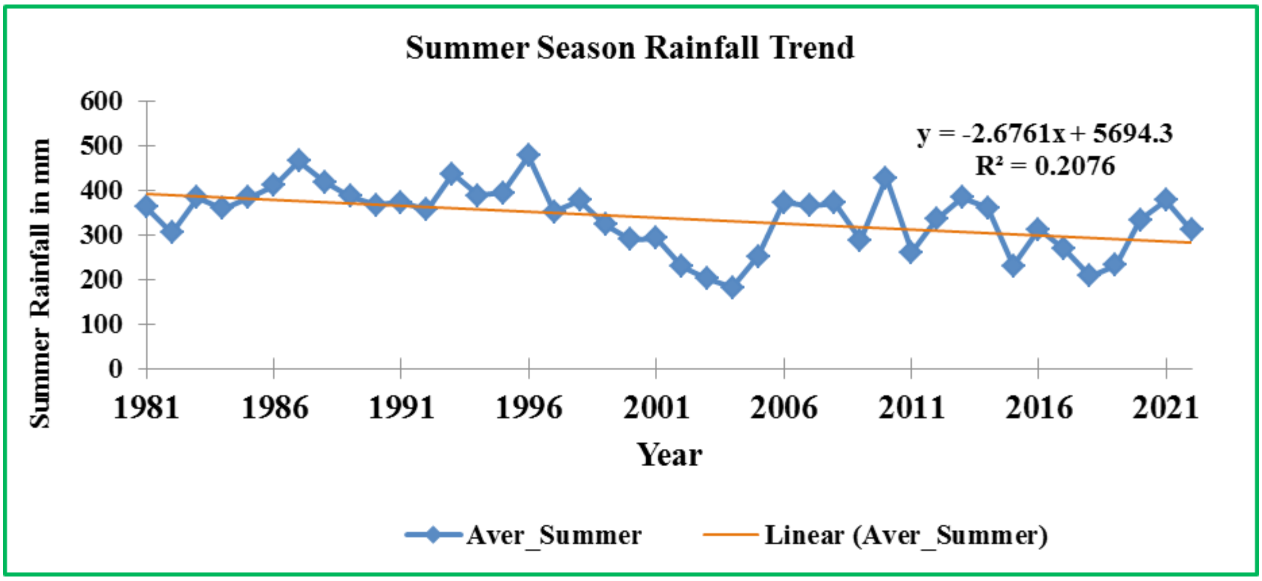

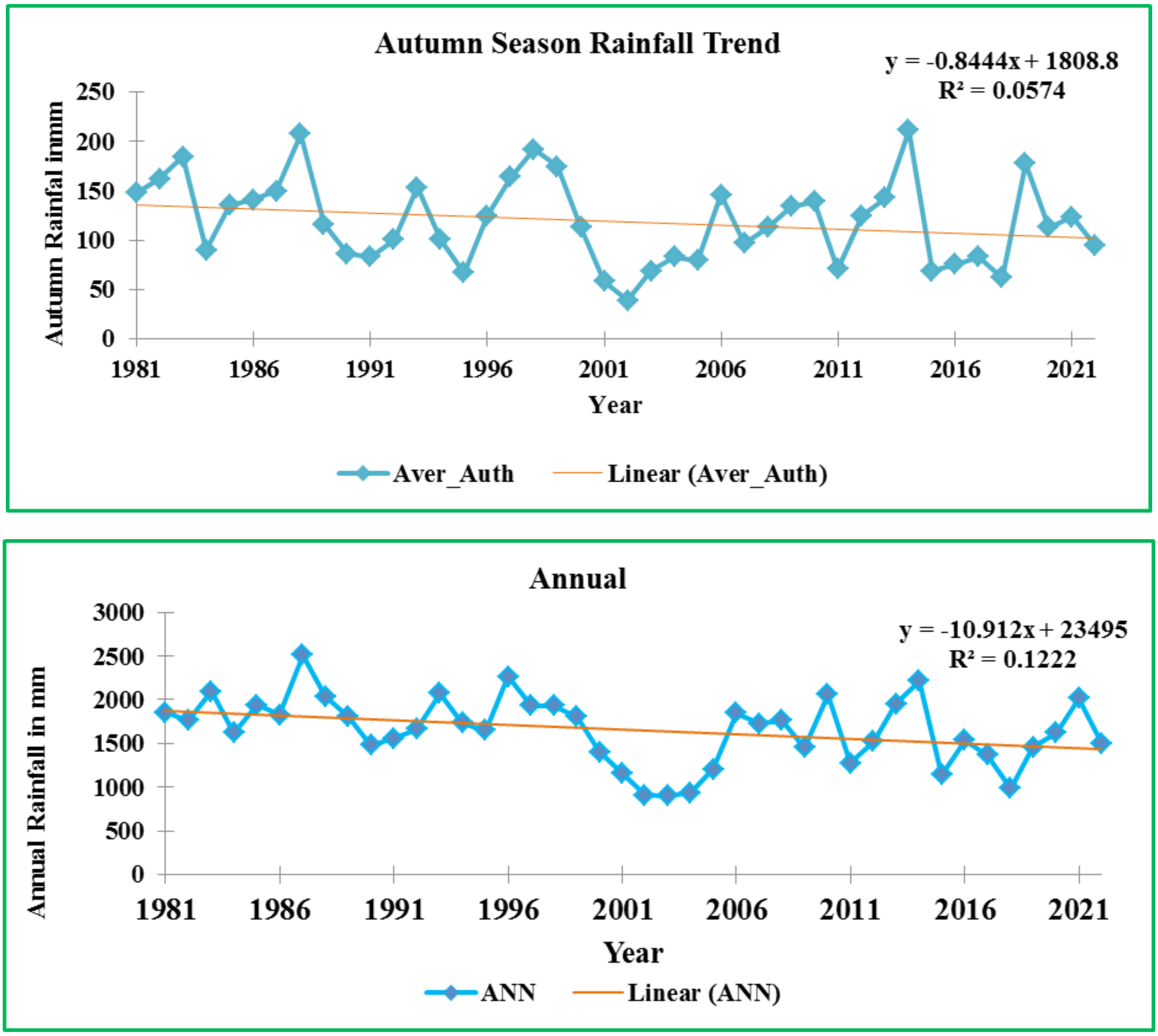

Figure 2. Winter, Spring, Summer, Autumn and annual rainfall trends

Table 3. Seasons and annual MK trend test result of temperature (1982-2022)

Seasons	Minimum	Maximum	Mean	Std. deviation	MK Test	Sen's Slope
Winter	26.767	31.740	28.820	1.300	0.389	14
Spring	30.507	34.880	32.774	1.126	0.500	18
Summer	23.850	27.010	25.285	0.845	0	0
Autumn	23.508	27.197	24.659	0.784	0.556	20
Annual	31.68	36.180	33.835	1.045	0.500	18

Source: Ethiopian Meteorological Agency (2022)

Temporal variability and trends of temperature

To investigate the temporal variations and trends, the mean seasonal minimum, maximum, and annual temperature data for the years 1981–2022 were shown Table 3 and Figure 3. The research area's lowest temperature was 23.5^{0}C, its highest temperature was 34.8^{0}C, and its yearly average was 33.8^{0}C Table 3. The yearly average, maximum, and lowest temperature regression coefficients Figure 3 indicated an increasing trend at 0.014^{0}C, 0.029^{0}C, and 0.037^{0}C, respectively. The average temperature for the winter, spring, summer, autumn, and decadal regression coefficient results all exhibited an increasing trend at rates of 0.049^{0}C, 0.039^{0}C, and 0.014^{0}C, 0.029^{0}C and 0.037^{0}C per decade, respectively Figure 3. More specifically, since the 2000s, there has been a sudden rise in temperature. In this case, it was discovered that the minimum temperature increased more quickly than the maximum. The rate of annual average, winter, spring, summer, and fall temperature has therefore grown by 0.189^{0}C, 0.215^{0}C, 0.184^{0}C, 0.042^{0}C, and 0.206^{0}C, respectively, over the last forty years (1981–2022). According to (McSweeney *et al.*, 2008; Asfaw *et al.*, 2018), these findings were supported. They came to the conclusion that many regions of Ethiopia have been seeing an increase in the annual, maximum, and minimum temperatures throughout all seasons.

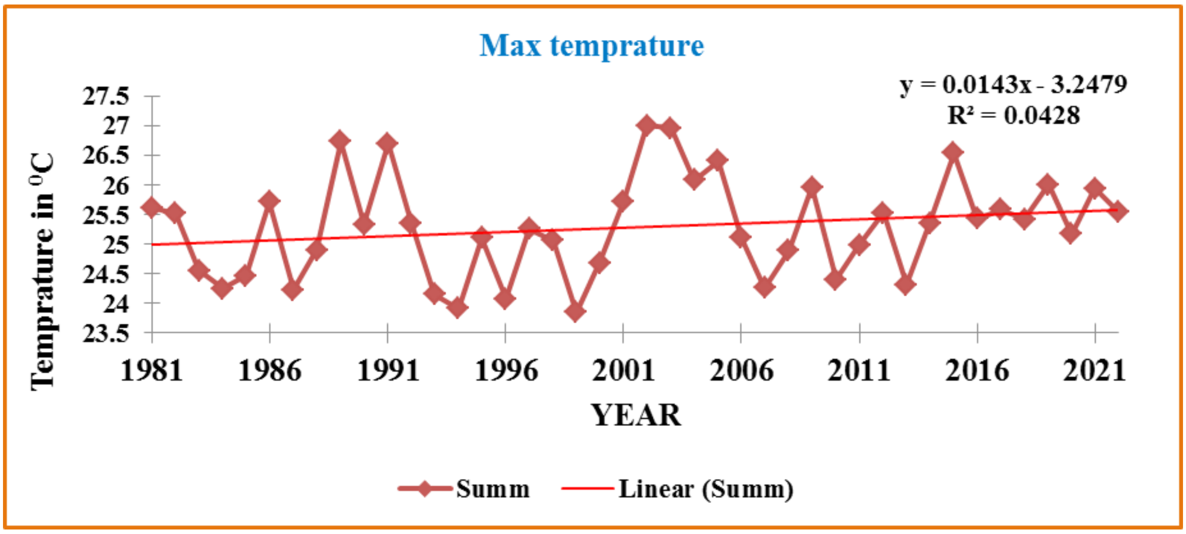
Max temprature
y = 0.0143x - 3.2479
R² = 0.0428
Temprature in ⁰C
27.5
27
26.5
26
25.5
25
24.5
24
23.5
1981
1986
1991
1996
2001
2006
2011
2016
2021
YEAR
Summ
Linear (Summ)

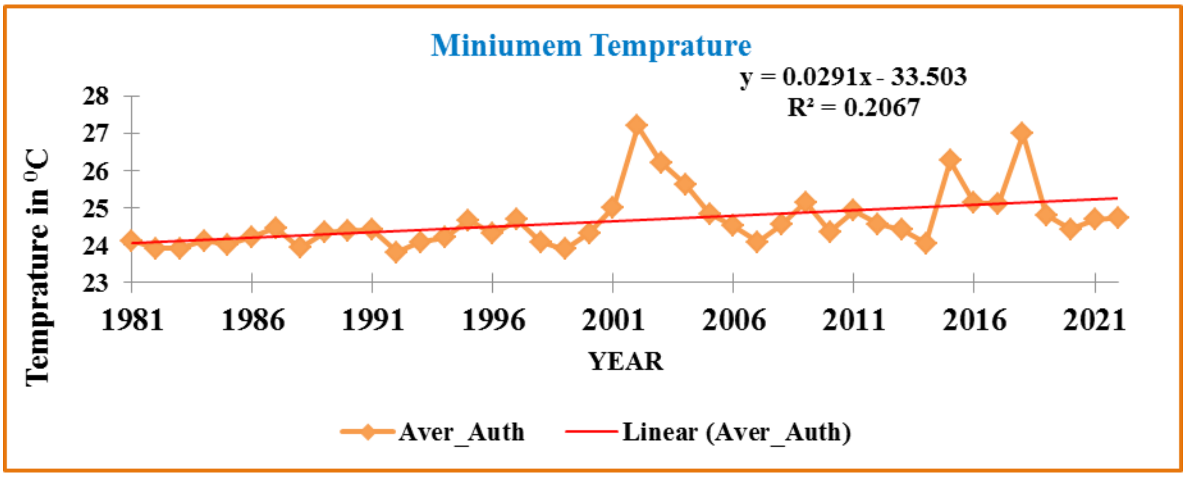
Miniumem Temprature
y = 0.0291x - 33.503
R² = 0.2067
Temprature in ⁰C
28
27
26
25
24
23
1981
1986
1991
1996
2001
2006
2011
2016
2021
YEAR
Aver_Auth
Linear (Aver_Auth)

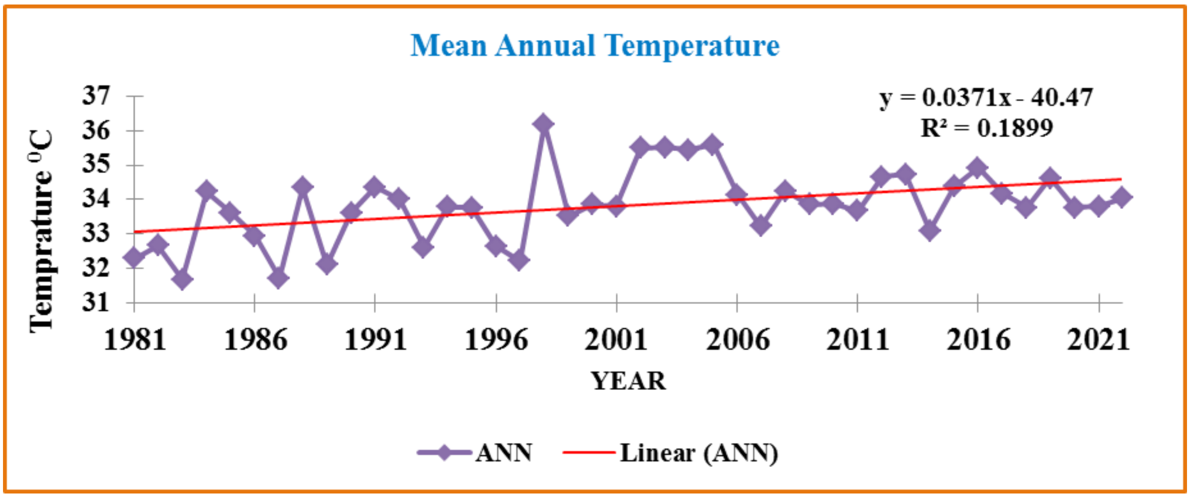
Mean Annual Temperature
y = 0.0371x - 40.47
R² = 0.1899
Temprature ⁰C
37
36
35
34
33
32
31
1981
1986
1991
1996
2001
2006
2011
2016
2021
YEAR
ANN
Linear (ANN)

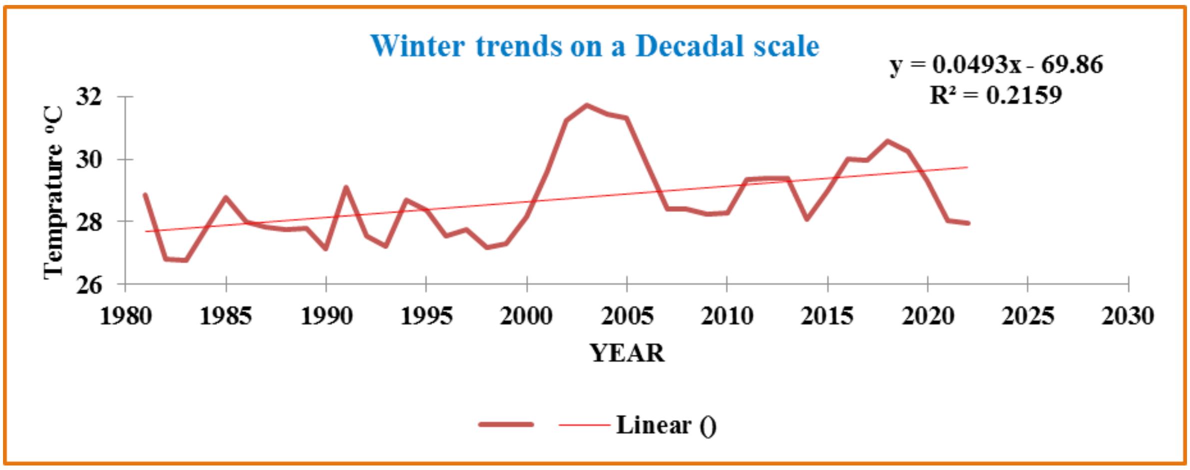
Winter trends on a Decadal scale
y = 0.0493x - 69.86
R² = 0.2159
Temprature ⁰C
32
30
28
26
1980
1985
1990
1995
2000
2005
2010
2015
2020
2025
2030
YEAR
Linear ()

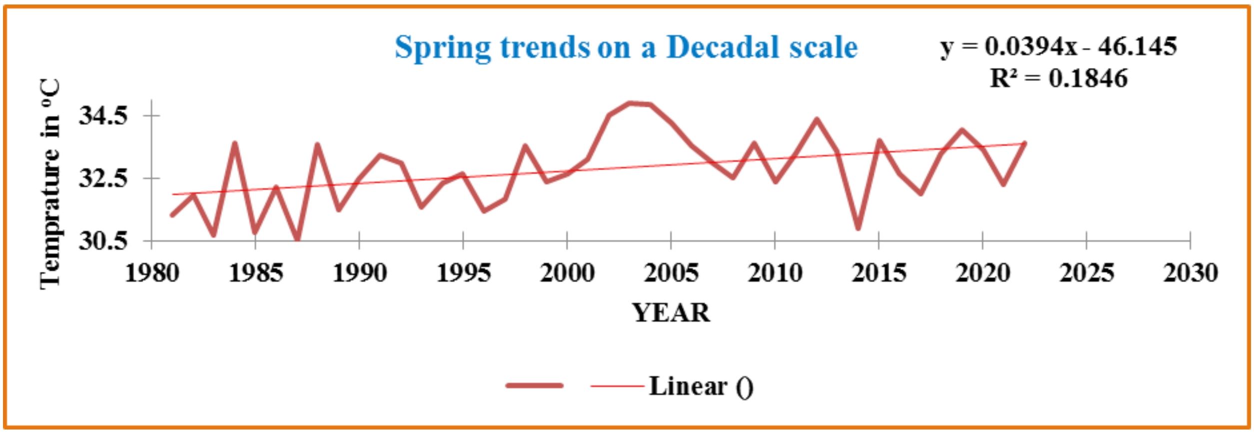

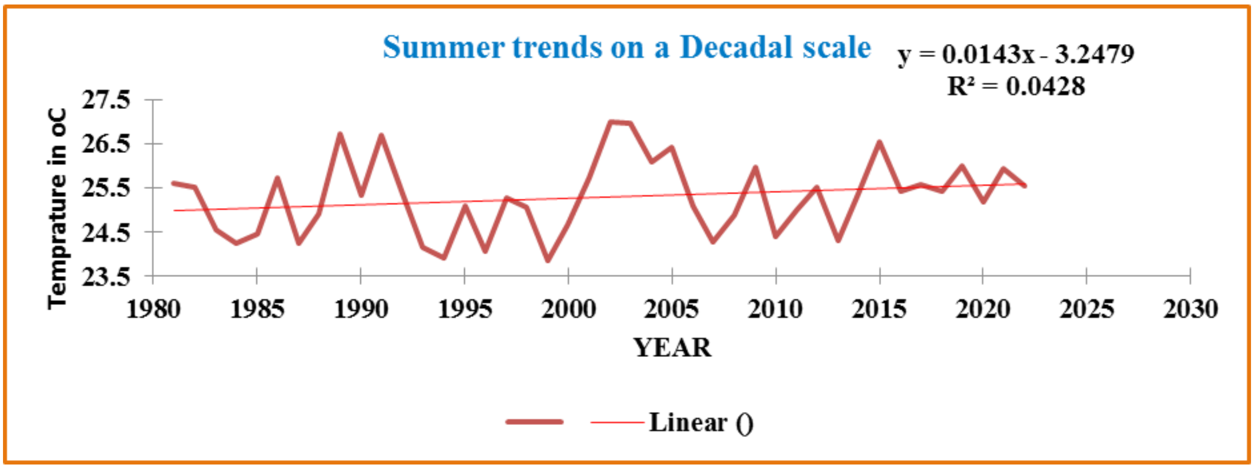

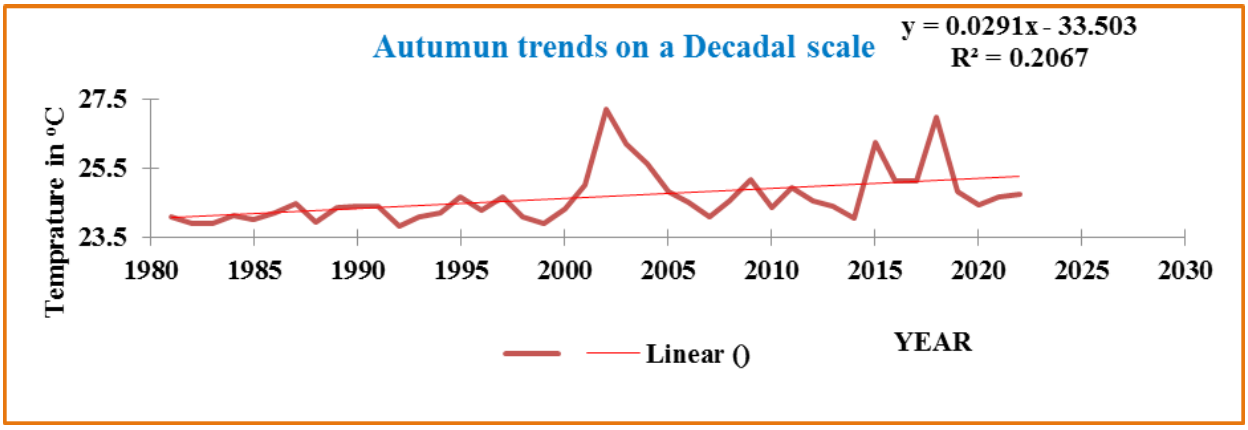

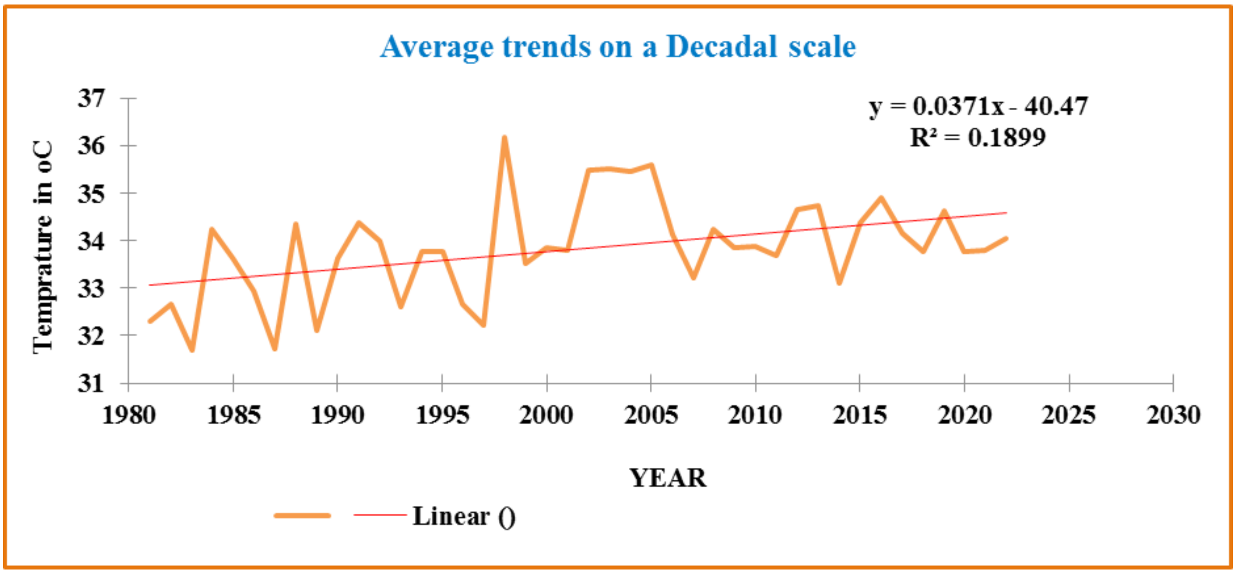

Figure 3. Decadal trends of winter, spring, summer, autumn and average temperature (1981-2022)

Spatial variability and trend of rainfall

Table 1 and Figure 4 showed the long-term spatial variability and trends of mean annual rainfall as well as spring, summer, autumn and winter rainfall. In comparison to the other areas, the upper portion of the district experienced the highest annual rainfall (1790–1890 mm/year). The district received rainfall ranging from 1768 mm to 1790 mm annually in more than 57% of cases. An additional 20% of the region experiences yearly precipitation ranging from 1790 to 1812 mm. Furthermore, a sizeable percentage of the district (13%) receives rainfall between 1746 and 1768 mm per year. The smallest amount of rainfall in the area, which ranges from 1702 to 1746 mm annually, falls on the remaining 10% of the district. The distribution of rainfall in space varies seasonally as well. For example, during the winter season (the dry season), the northeastern part of the district receives 8.35 to 8.57 mm (5%) of rainfall on a seasonal basis; this is the driest season in the district. The northeastern part also receives 8.57 to 8.71 mm (10%) of rainfall per season, the north and northwest receives 8.71 to 8.82 mm (20%) of rainfall per season, and the rest of the district receives 8.82 to 8.9 mm (25%) of rainfall the southwest section of the area receives 8.9 to 8.99 mm (40%) of rainfall every season, compared to the southeast and south.

The district experiences varying amounts of rainfall during the spring season, which is the small rainy season. Seasonally, the northeastern part of the district receives 5% of the rainfall, while the north and northwest parts receive 10%, 82.81 to 83.87 mm, and the north and northwest parts receive 20%. Additionally, the south and central parts receive 25% of the rainfall, and the south, central, and southeast parts receive 40% of the rainfall. The district experiences varying amounts of rainfall during the spring season, which is the small rainy season. Seasonally, the northeastern part of the district receives 5% of the rainfall, while the north and northwest parts receive 10%, 82.81 to 83.87 mm, and the north and northwest parts receive 20%. Additionally, the south and central parts receive 25% of the rainfall, and the south, central, and southeast parts receive 40% of the rainfall. According to this, the district is nearly completely covered by the 375.78mm to 379.12mm (80%) of rainfall that falls throughout the summer, the major rainy season. The district's summer rainfall is distributed as follows: the south and southwest receive 372.44 to 375.78 mm (25%) of the total rainfall, the western part receives 369.11 to 372.44 mm (20%) of the total rainfall per season, the western part receives 365.77 to 369.11 mm (10%) of the total rainfall, and the southwestern part receives 362.43 to 365.77 mm (5%) of the total rainfall in each of the district's three agro-ecological zones.

Autumn is the district's small rainy season. Seasonally, the district receives between 124.66 and 126.53 mm of rainfall in the north and northwest tip; from the northwestern tip to the northeastern part of the district, between 126.53 and 128.39 mm of rainfall; from the northwestern tip to the northeastern part of the district, between 128.39 and 130.26 mm of rainfall in the north and northwest part of the district per season; from the southern tip and western part of the district, 130.26 to 132.13 mm of rainfall received; from the central and southwestern part of the district, between 132.31 and 133.99 mm of rainfall received per season (Gebrehiwot *et al.*, 2011; Ayalew *et al.*, 2012; UNFCCC, 2015; Z. Y. Alemayehu *et al.*, 2022) all reported findings that were similar.

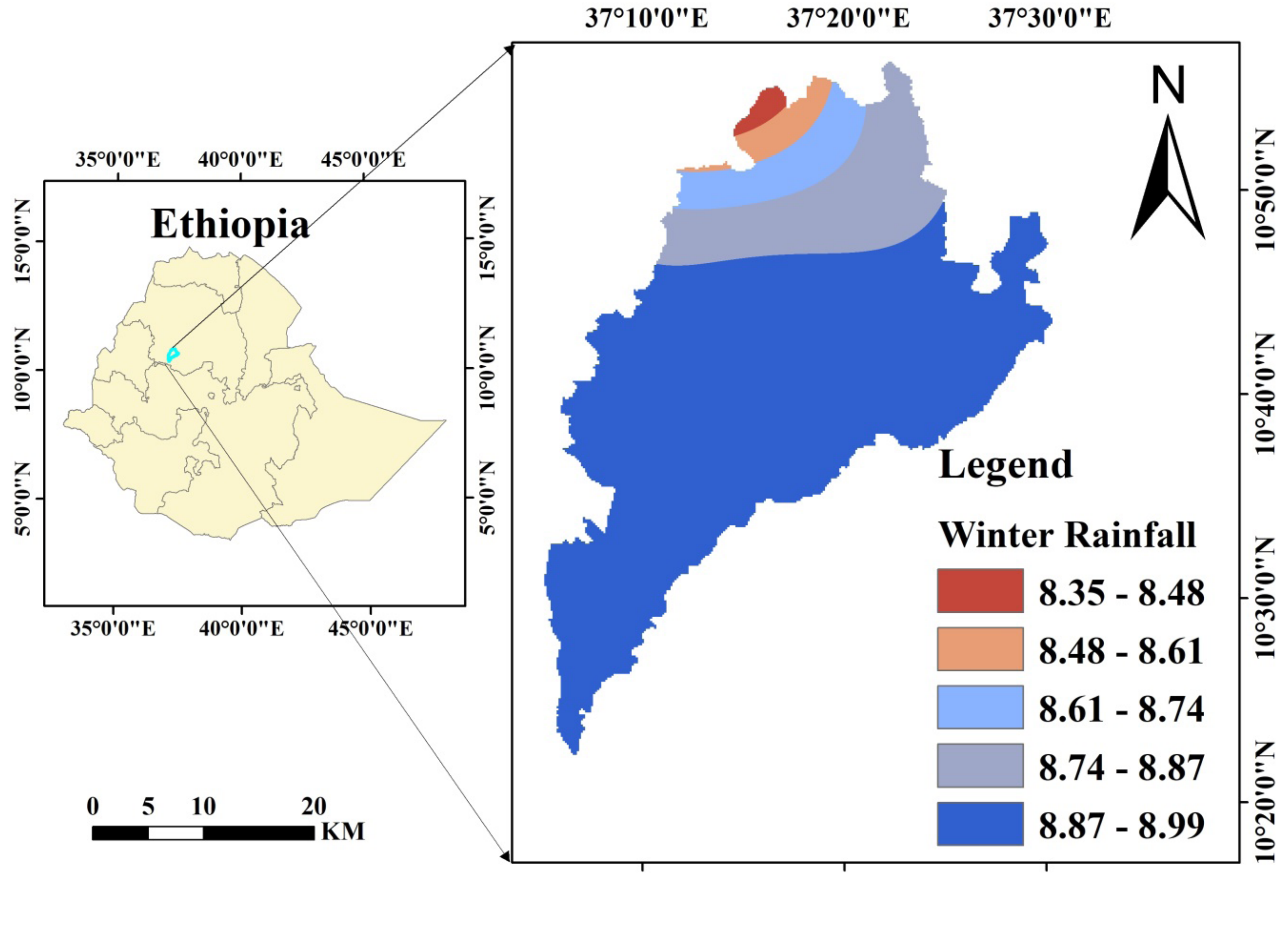

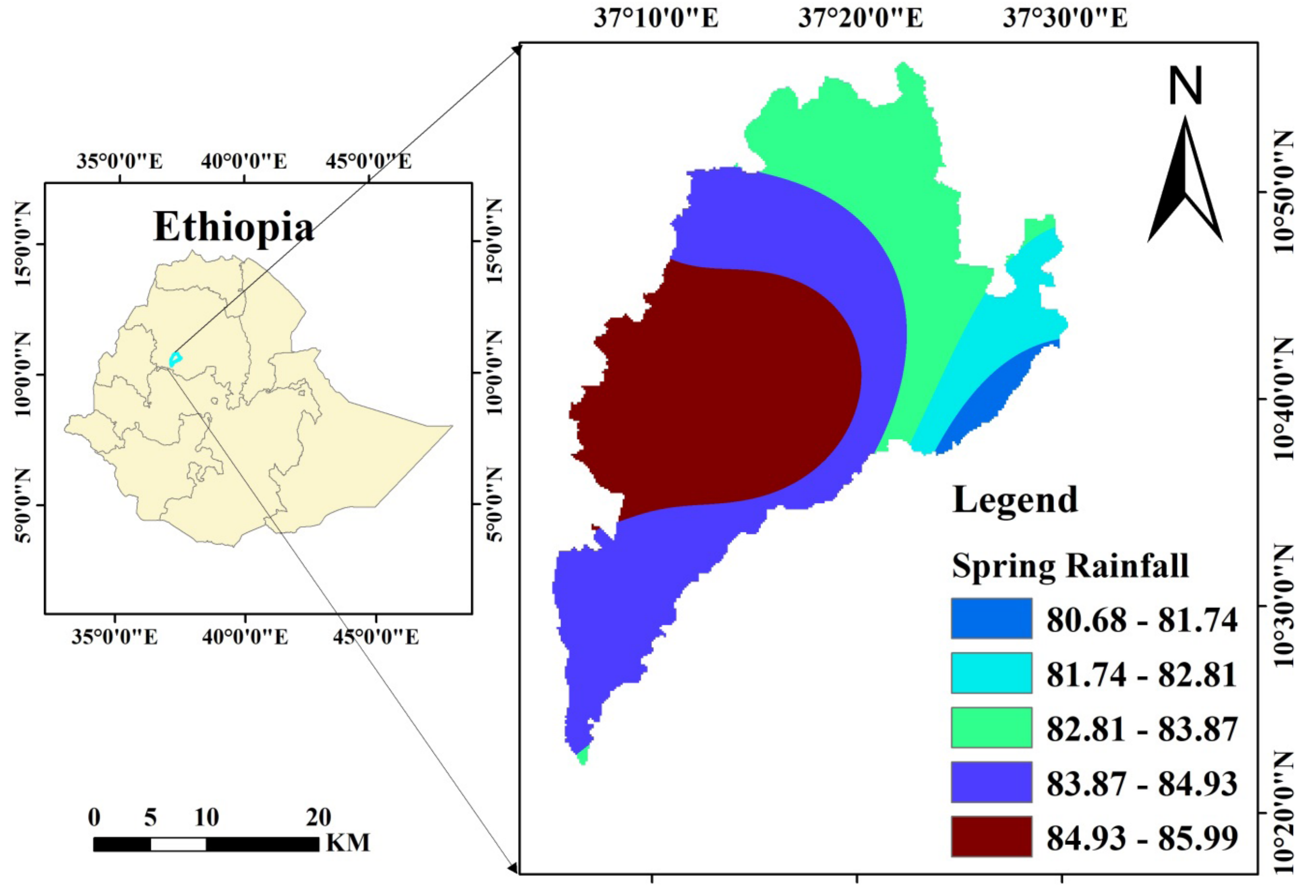
37°10'0"E
37°20'0"E
37°30'0"E
35°0'0"E
40°0'0"E
45°0'0"E
Ethiopia
15°0'0"N
10°0'0"N
5°0'0"N
N
10°50'0"N
10°40'0"N
10°30'0"N
10°20'0"N
Legend
Spring Rainfall
80.68 - 81.74
81.74 - 82.81
82.81 - 83.87
83.87 - 84.93
84.93 - 85.99
0 5 10 20
KM

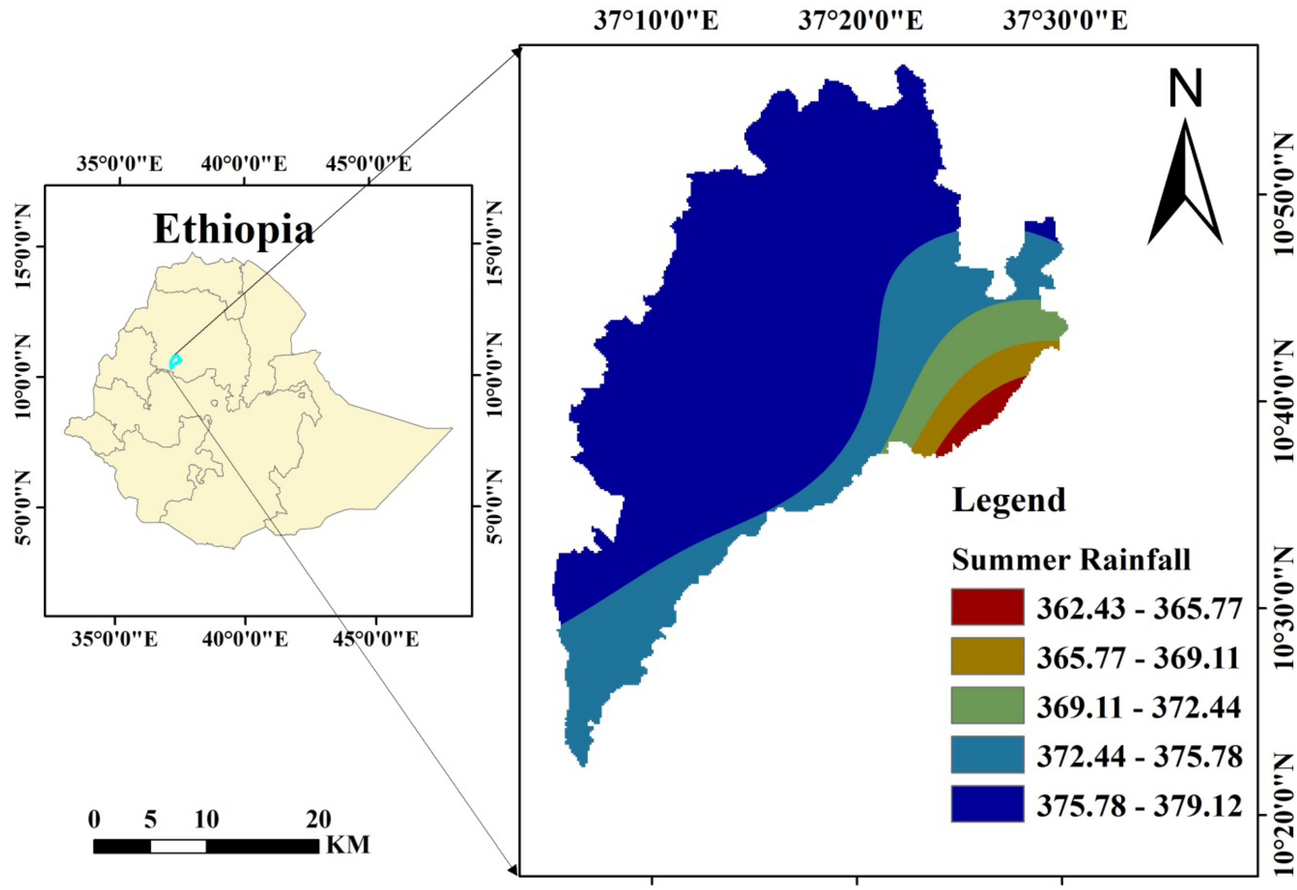
37°10'0"E
37°20'0"E
37°30'0"E
35°0'0"E
40°0'0"E
45°0'0"E
Ethiopia
15°0'0"N
10°0'0"N
5°0'0"N
N
10°50'0"N
10°40'0"N
10°30'0"N
10°20'0"N
Legend
Summer Rainfall
362.43 - 365.77
365.77 - 369.11
369.11 - 372.44
372.44 - 375.78
375.78 - 379.12
0 5 10 20
KM

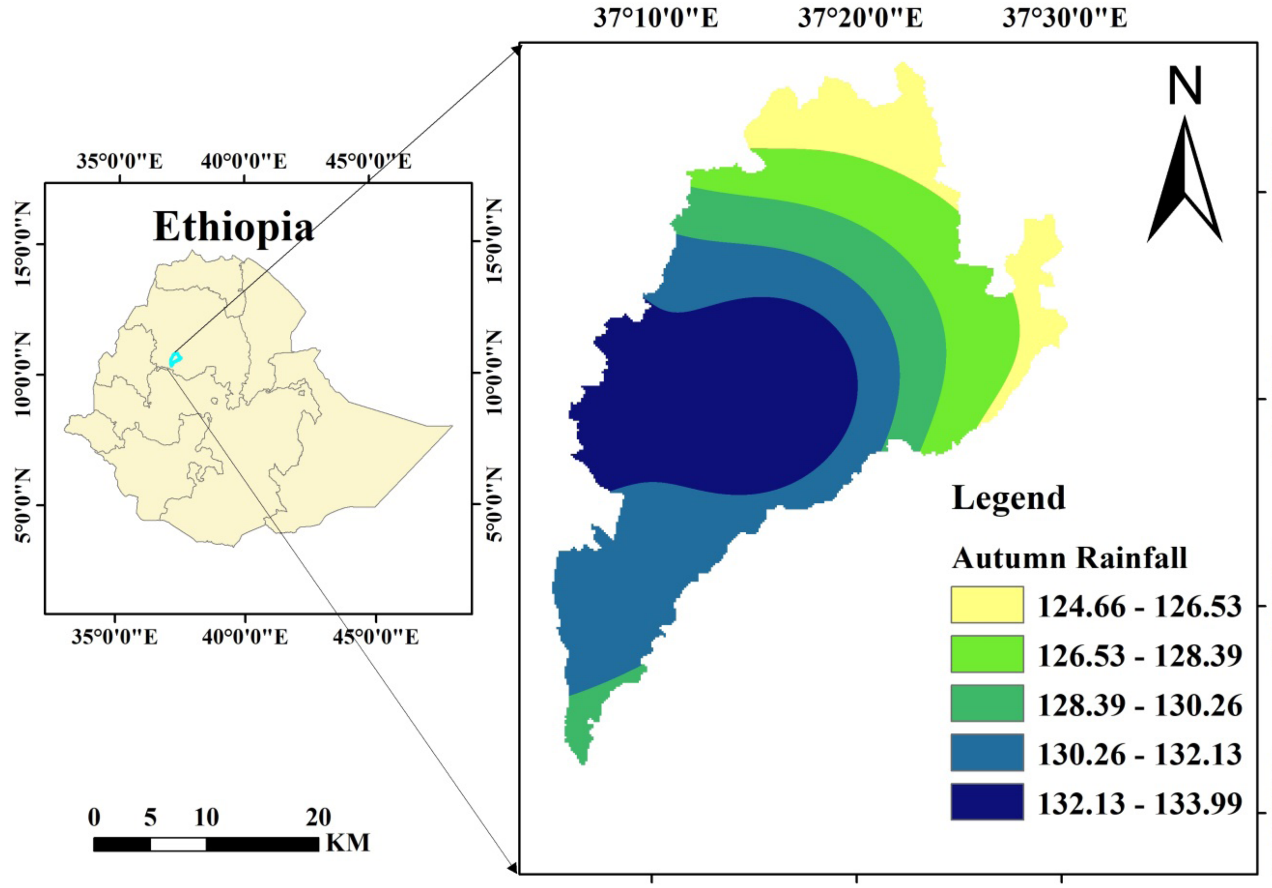

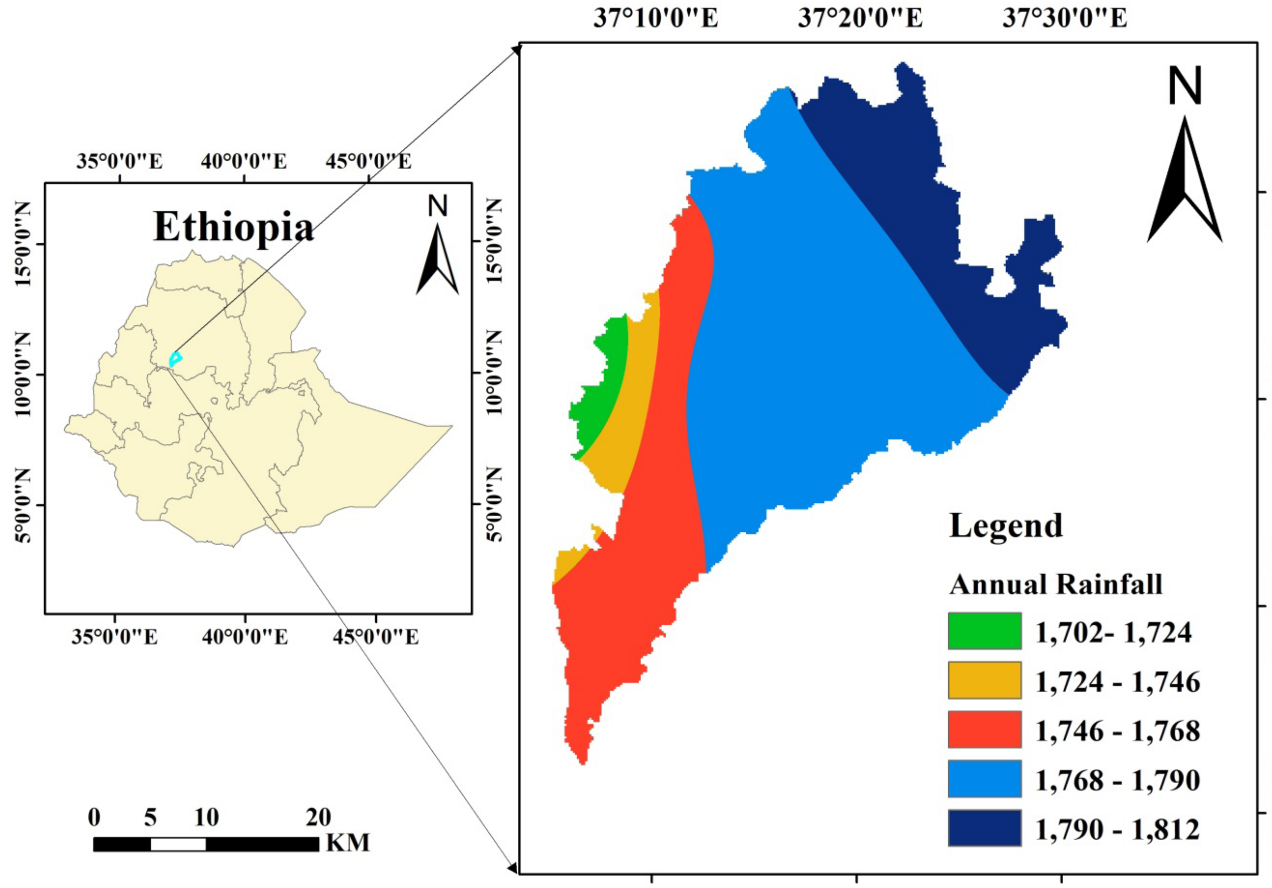

Figure 4. Spatial trends of winter, spring, summer, autumn and annual rainfall (1981-2022)

Spatial variability and trend of temperature

Table 3 and Figure 5 show the long-term spatial variability and trends of the mean annual temperature as well as the temperatures in the spring, summer, autumn and winter. The annual spatial temperature distribution was as follows: the northeastern part of the district receives temperatures between 22.49⁰C and 25.44⁰C (5%), the northeastern part receives temperatures between 25.44⁰C and 27.34⁰C (10%), the north and northwest receives temperatures between 27.34⁰C and 28.9⁰C (20%), the rest of the district receives temperatures between 28.9⁰C and 30.32⁰C (25%) and the southwest receives temperatures between 30.32⁰C and 31.9⁰C (40%).

Seasonal variations in the spatial distribution of temperature also occur. For example, the maximum temperature experienced seasonally in the northeastern section of the area was 27.06⁰C to 27.79⁰C (10%), while the winter season temperature ranges from 26.33⁰C to 27.06⁰C (5%). Additionally, the maximum temperature received by the northeastern portion of the district is between 27.79⁰C and 28.53⁰C (20%), while the north and northwest portion of the district receives maximum temperatures between 28.53⁰C and 29.26⁰C (25%) and the rest of the central, south, and southeast portion receives maximum temperatures between 29.26⁰C and 29.99⁰C (40%). The spring season's maximum temperature, as shown in Figure 5, varies in space from 29.5⁰C to 30.4⁰C (5%), indicating a seasonally significant increase in the maximum temperature received in the northeastern part of the district; additionally, the northeastern part of the district receives maximum temperatures between 30.4⁰C and 31.3⁰C (10%), 31.3⁰C and 32.2⁰C (20%), 32.32⁰C and 33.1⁰C (25%), and the rest of the central, south, and southeast part of the district receives maximum temperatures between 33.1⁰C and 33.9⁰C (40%), and 33.1⁰C and 33.9⁰C (45%) of the maximum temperature received in the southwest part of the district.

The highest temperature in the summer ranges from 23.27⁰C to 23.82⁰C (5%). Seasonally, the northeastern region of the area experiences high temperatures between 23.82⁰C and 24.36⁰C (10%). The northeastern region of the district experiences maximum temperatures ranging from 24.36⁰C to 24.91⁰C (20%) depending on the season. maximum temperature received by the district's northwest and northwestern regions is between 24.91⁰C and 25.45⁰C (25%) of the maximum temperature received by the rest of the district's central, south, and southeast regions, and between 25.45⁰C and 25.99⁰C (40%) of the maximum temperature received by the southwest region. The highest temperature was in the autumn ranges from 22.27⁰C to 22.82⁰C (5%). Seasonally, the northeastern region of the area experiences high temperatures between 22.82⁰C and 23.36⁰C (10%). The Northeastern Part District experienced a maximum temperature of 23.36⁰C to 23.91⁰C (20%) per season. maximum temperature received by the district's north and northwest, which ranges from 23.91⁰C to 24.45⁰C (25%) of the maximum temperature received by the rest of the district's central, south, and southeast, and which ranges from 24.45⁰C to 24.99⁰C (40%) of the maximum temperature received by the district's south west. The findings aligned with the research conducted by (Teyso *et al.*, 2016; Suryabhagavan & extremes, 2017; Asfaw *et al.*, 2018).

The northeastern region of the district receives an annual minimum temperature distribution of 4.6⁰C to 6⁰C (5%), while the southeast receives an annual minimum temperature distribution of 6⁰C to 6.8⁰C (10%). The northern region of the district likewise experiences a minimum temperature of 6.8⁰C to 7.5⁰C (20%) annually. Minimum temperatures are received in the south and southwest of the district annually, in the outer shell of the central district annually between 7.5⁰C and 8.2⁰C (25%) and in the central section of the district annually between

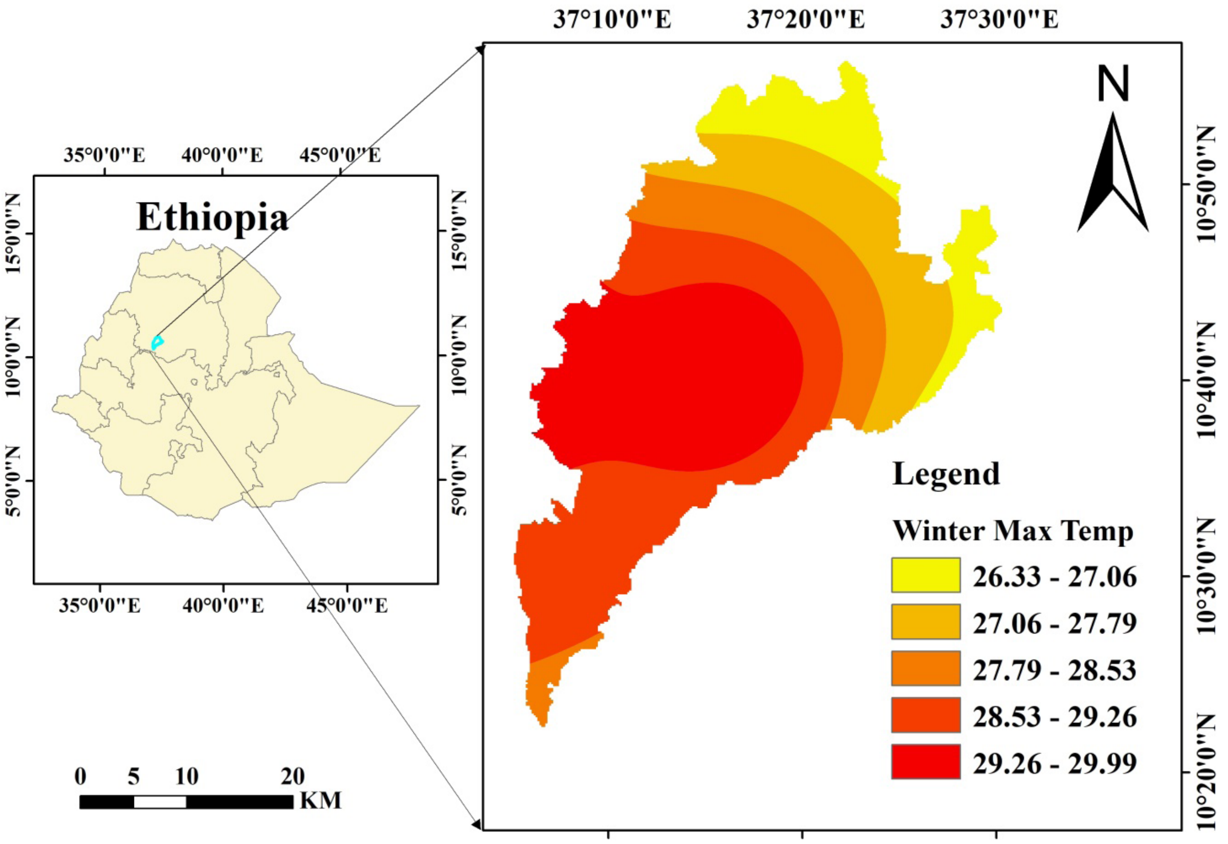

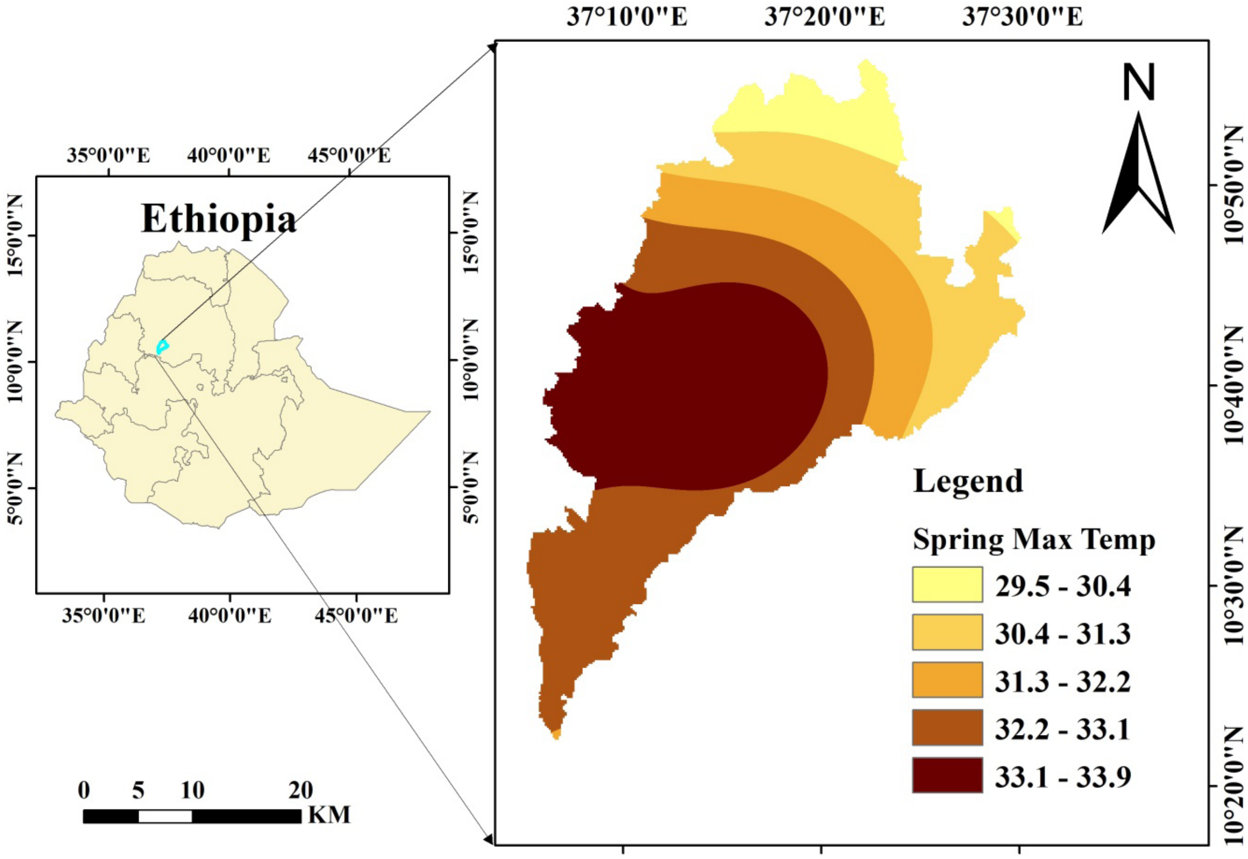
Ethiopia
35°0'0"E
40°0'0"E
45°0'0"E
15°0'0"N
10°0'0"N
5°0'0"N
0 5 10 20 KM
37°10'0"E
37°20'0"E
37°30'0"E
10°50'0"N
10°40'0"N
10°30'0"N
10°20'0"N
N
Legend
Spring Max Temp
29.5 - 30.4
30.4 - 31.3
31.3 - 32.2
32.2 - 33.1
33.1 - 33.9

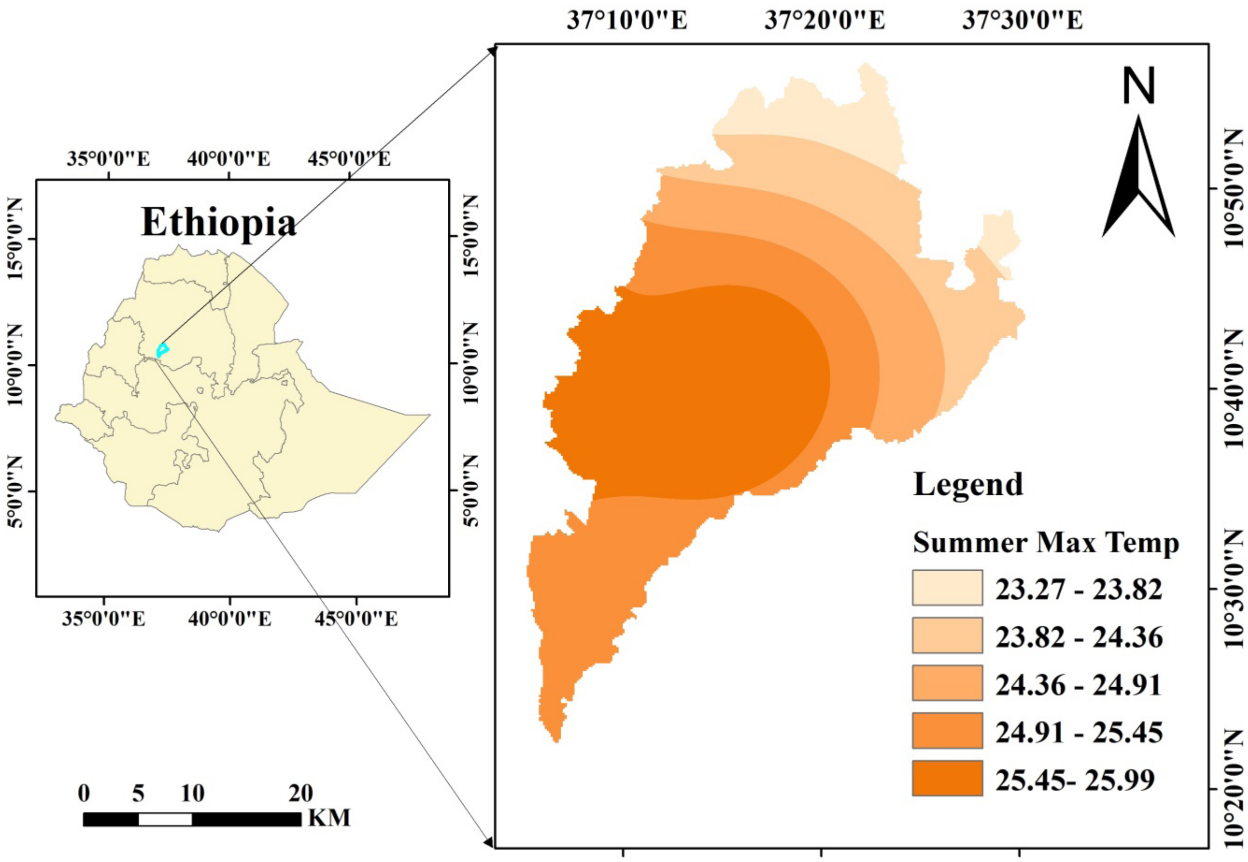
Ethiopia
35°0'0"E
40°0'0"E
45°0'0"E
15°0'0"N
10°0'0"N
5°0'0"N
0 5 10 20 KM
37°10'0"E
37°20'0"E
37°30'0"E
10°50'0"N
10°40'0"N
10°30'0"N
10°20'0"N
N
Legend
Summer Max Temp
23.27 - 23.82
23.82 - 24.36
24.36 - 24.91
24.91 - 25.45
25.45- 25.99

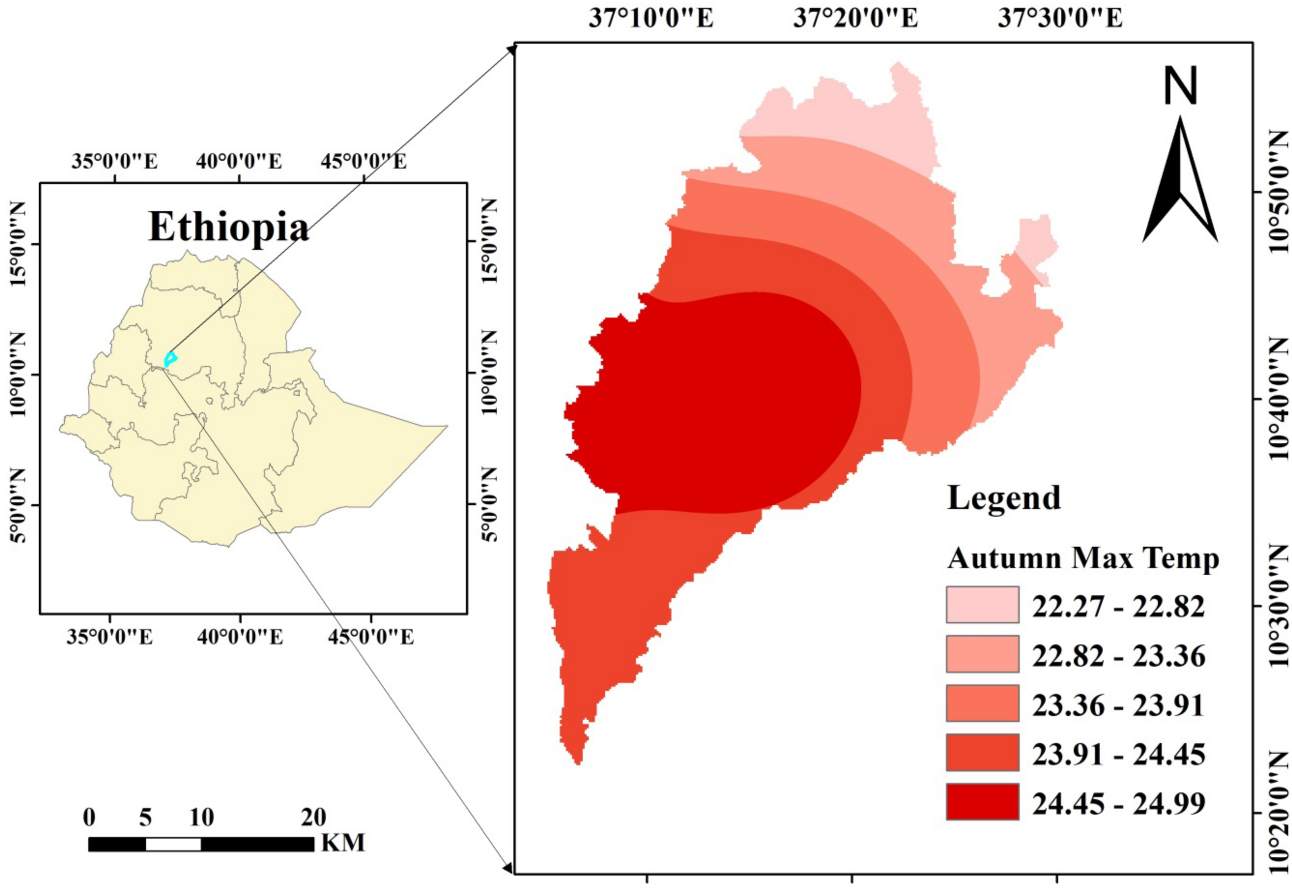

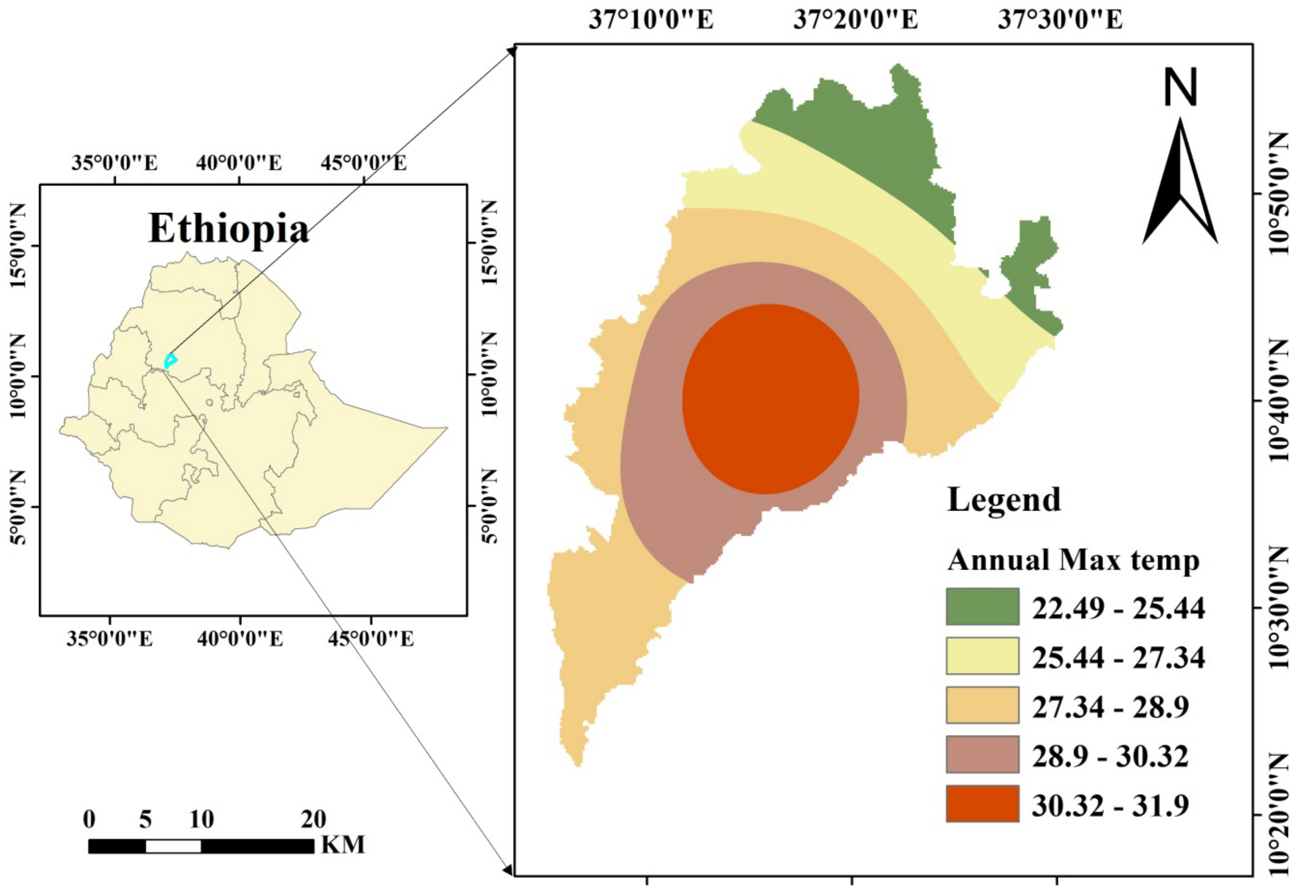

Figure 5. Spatial trends of maximum temperature for seasons and annual from (1981-2022)

8.2⁰C and 8.9⁰C (40%). In the winter which is the coolest season, the minimum temperature ranges from 7.24⁰C to 7.79⁰C (5%). The northeastern region of the district experiences a seasonal minimum temperature range of 7.79⁰C to 8.34⁰C (10%). Additionally, the northeastern portion of the district receives temperature readings from 8.34⁰C to 8.89⁰C (20%), the north and northwest portion of the district receives 8.89⁰C to 9.44⁰C (25%) of minimum temperature readings, and the rest of the central, south, and southeast portion of the district records 9.44⁰C to 9.99⁰C (40%) of minimum temperature readings. Based on the data presented in Figure 6, it can be observed that the minimum temperature in the spring varies in space from 11⁰C to 11.65⁰C (5%). This indicates a seasonally increasing trend in minimum temperature received by the northeastern part of the district, from 11.65⁰C to 12.24⁰C (10%), and from 12.24⁰C to 12.82⁰C (20%) in the north and northwest regions of the district each season, with the remaining centre, south, and southeast regions receiving 12.82⁰C to 13.41⁰C (25%) of the minimum temperature and the southwest region receiving 13.41⁰C to 13.99⁰C (40%) of the minimum temperature.

The minimum temperature in the summer ranges from 11.24⁰C to 11.94⁰C (5%). Seasonally, the northeastern region of the district experiences minimum temperatures between 11.94⁰C and 12.49⁰C (10%). The northeastern region of the district experiences minimum temperatures ranging from 12.49⁰C to 13.01⁰C (20%) depending on the season. Minimum temperatures are received in the north and northwestern parts of the district per season; the rest of the central, south, and southeast parts of the district receive minimum temperatures between 13.01⁰C and 13.46⁰C (25%) and the south west part of the district receives minimum temperatures between 13.46⁰C and 13.99⁰C (40%) per season. The minimum temperature throughout the autumn season ranges from 7.67⁰C to 8.45⁰C (5%). Seasonally, the north-east portion of the district experiences minimum temperatures between 8.45⁰C and 9⁰C (10%), and throughout the district season, minimum temperatures between 9⁰C and 9.6⁰C (20%). minimum temperature received by the district's north and northwest each season; 9.6⁰C to 10⁰C (or 25%) of minimum temperature received by the remaining central, south, and southeast regions each season; and 10⁰C to 10.7⁰C (or 40%) of minimum temperature received by the district's southeast region Figure 6. In the eastern and northeastern regions of the country, the minimum temperature showed a combination of significant declining and non-significant trends, yielding the same result across different regions Figure 6.

Discussion

Rainfall distribution and erratic rainfall distribution (49.5%), the statistical analysis reveals that there is a range of variability in spatiotemporal rainfall and temperature within the district (Mekonen *et al.*, 2020). This variability spans from moderate to high levels, both seasonally and annually. As an example, rainfall exhibited high variability (CV > 36.4) in the district during the autumn, winter and spring seasons, while it showed moderate variability during the annual and summer seasons (CV 21.3 to 23.1) (Yekoy, 2022) also found there was a greater variation noted during the autumn and winter seasons in comparision to the yearly and summer period (Sharma *et al.*, 2024). Further research findings indicated that there was greater rainfall variability noted throughout the autumn, spring and winter period comparision to the summer period in the northeastrn highlands,north eastrn ethiopia,westrn ethiopia and northwest parts of Ethiopia (Alemayehu *et al.*,

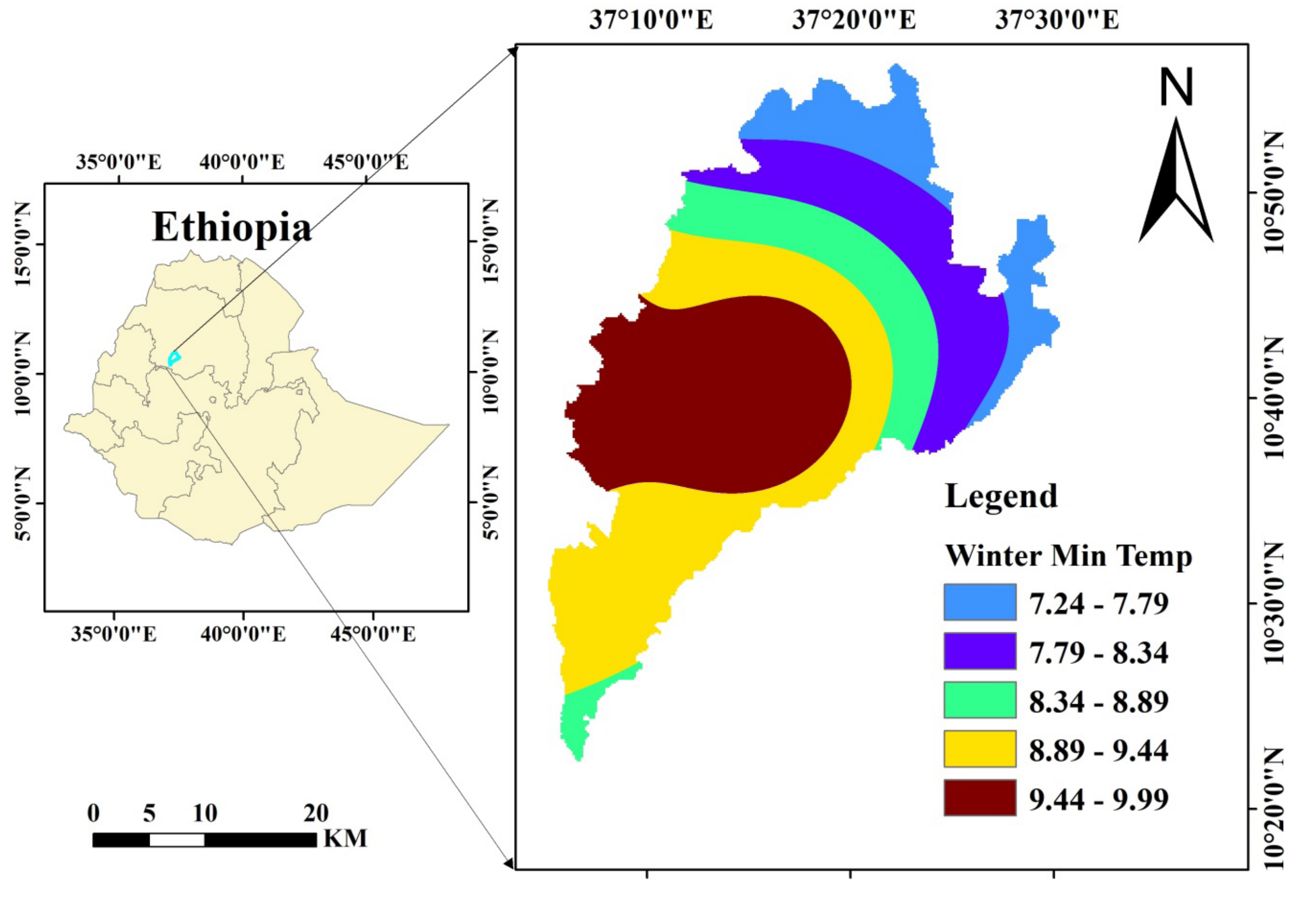

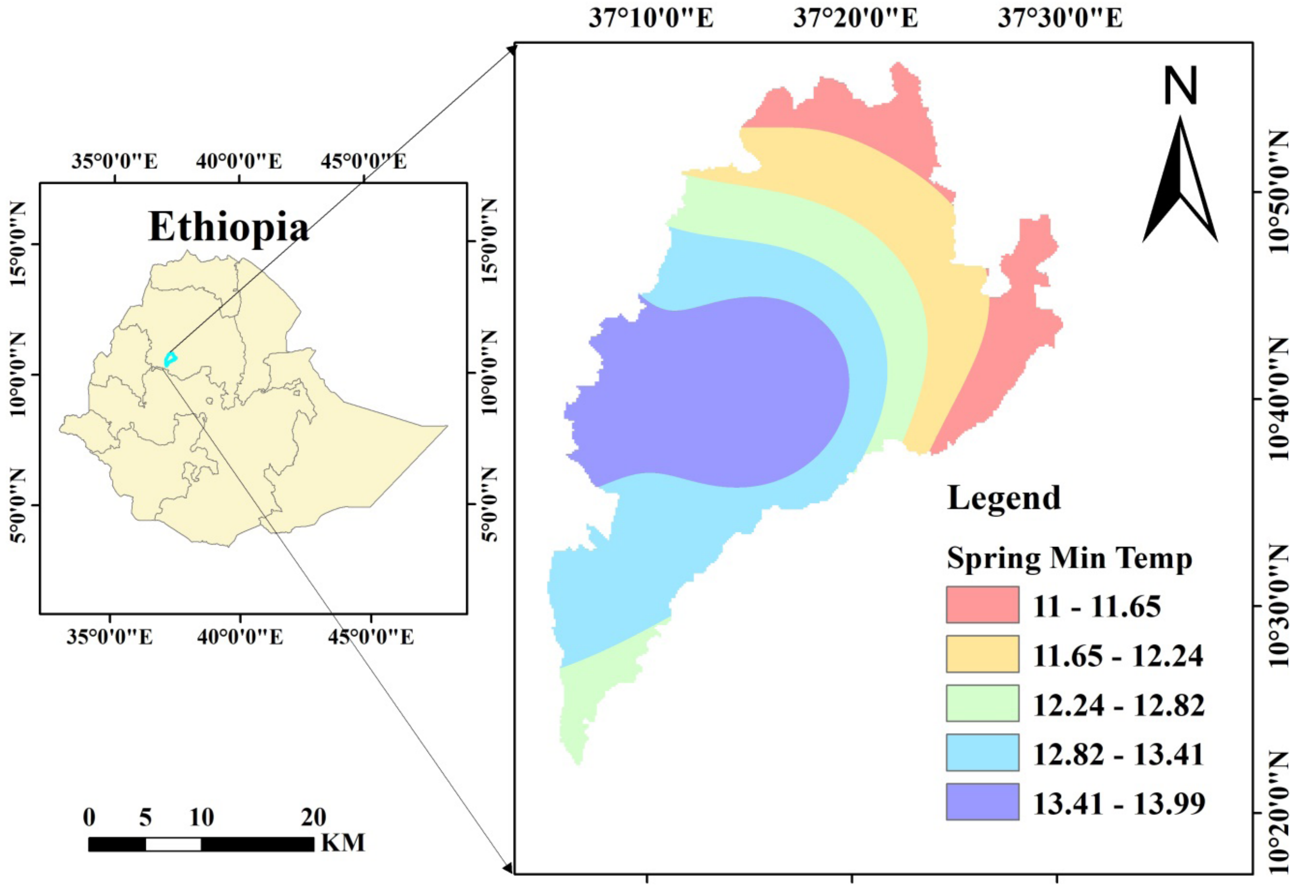
37°10'0"E
37°20'0"E
37°30'0"E
10°50'0"N
10°40'0"N
10°30'0"N
10°20'0"N
N
Ethiopia
35°0'0"E
40°0'0"E
45°0'0"E
15°0'0"N
10°0'0"N
5°0'0"N
0 5 10 20
KM
Legend
Spring Min Temp
11 - 11.65
11.65 - 12.24
12.24 - 12.82
12.82 - 13.41
13.41 - 13.99

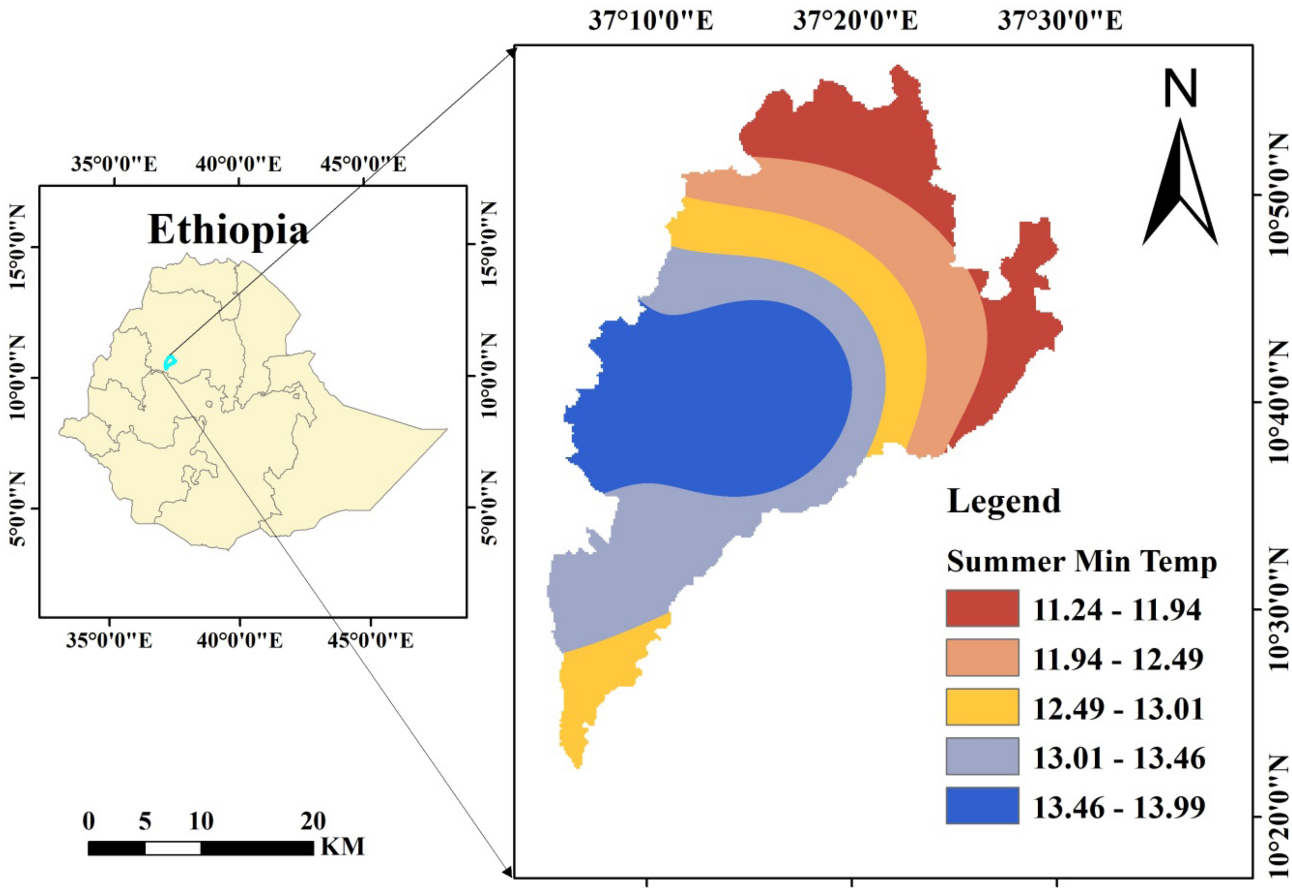
37°10'0"E
37°20'0"E
37°30'0"E
10°50'0"N
10°40'0"N
10°30'0"N
10°20'0"N
N
Ethiopia
35°0'0"E
40°0'0"E
45°0'0"E
15°0'0"N
10°0'0"N
5°0'0"N
0 5 10 20
KM
Legend
Summer Min Temp
11.24 - 11.94
11.94 - 12.49
12.49 - 13.01
13.01 - 13.46
13.46 - 13.99

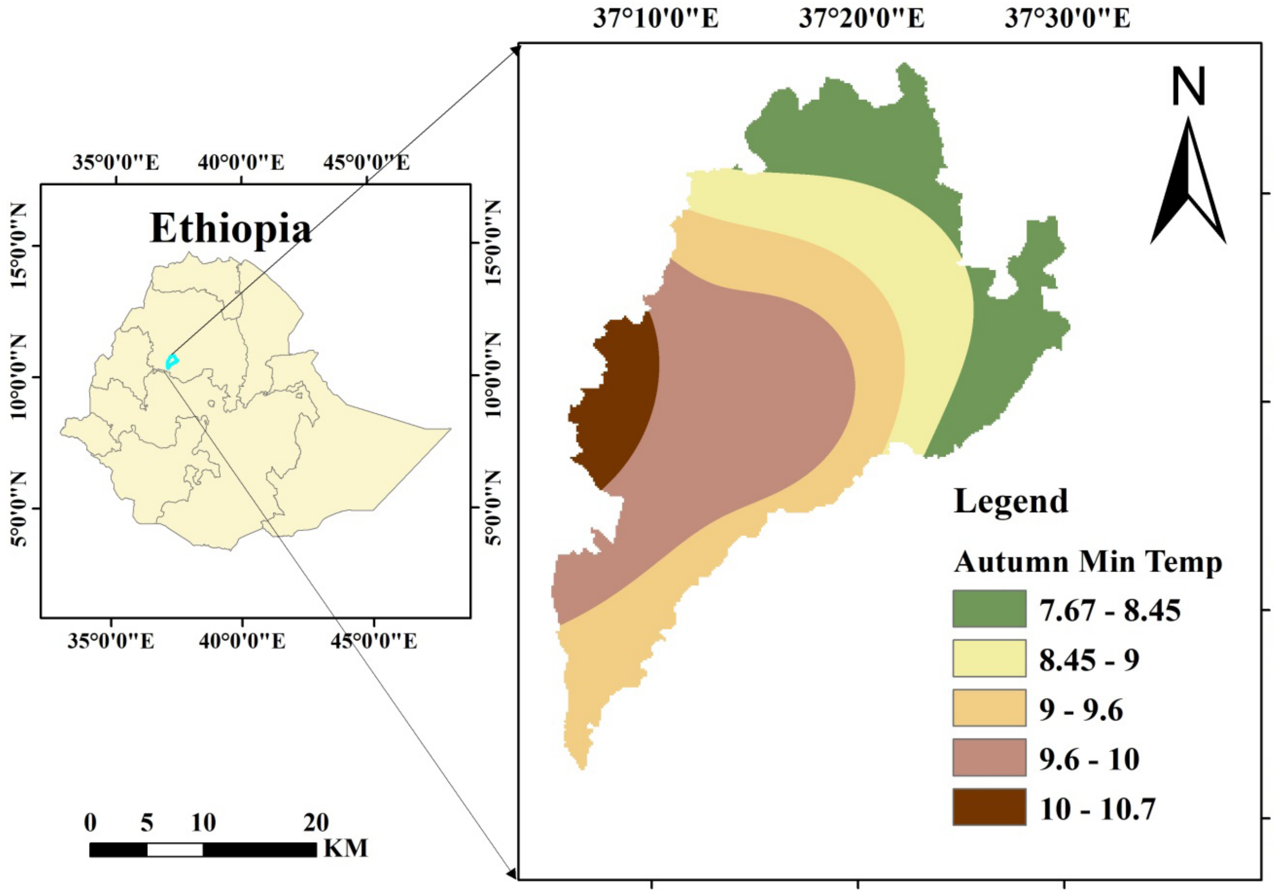

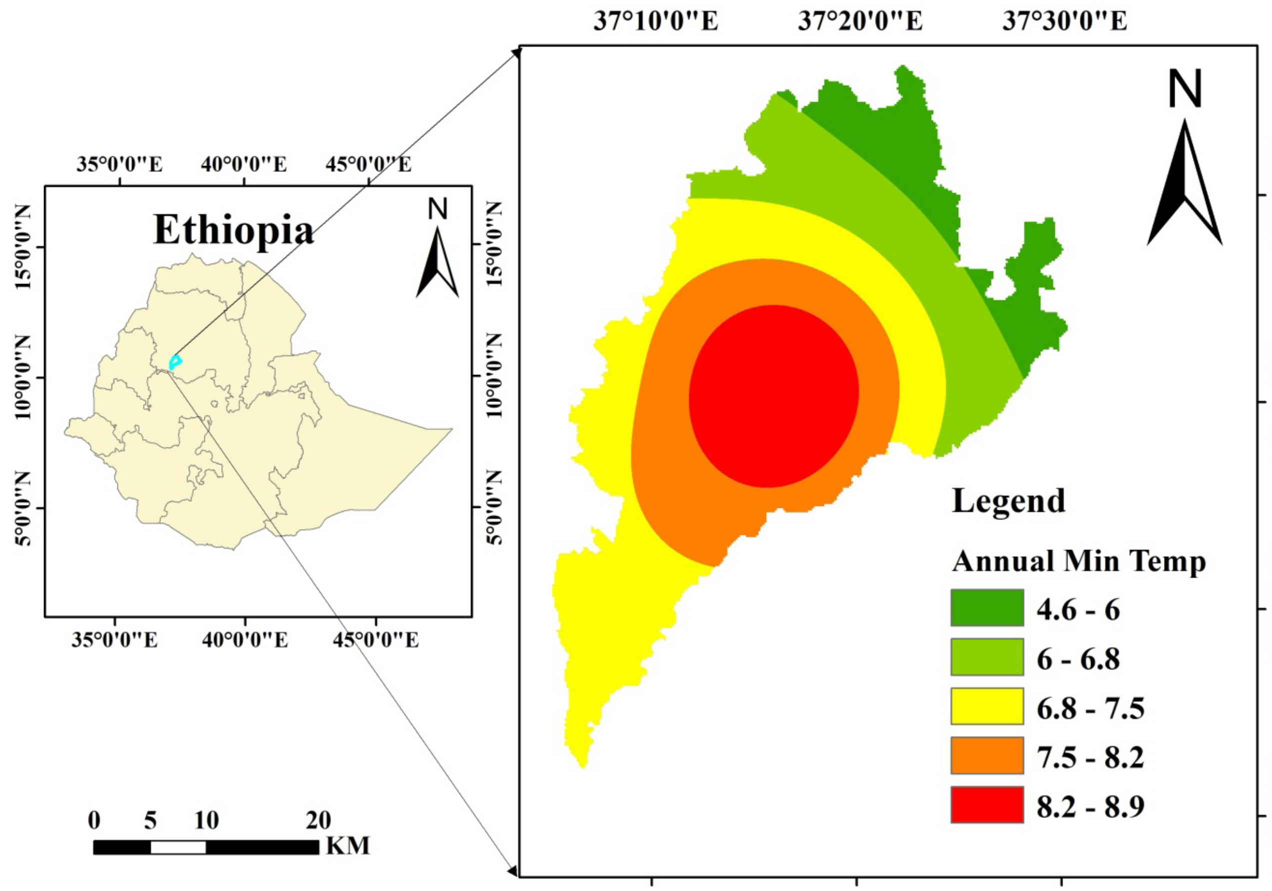

Figure 6. Spatial trends of minimum temperature for seasons and annual from (1981-2022)

2020a; Bahiru *et al.*, 2020; Wassie *et al.*, 2022; Yekoy, 2022). The mankendall trend test indicated that seasonal (winter, summer, autumn) annual rainfall exhibited a slight decreasing trend, while a significant declining trend was observed for spring season rainfall (Woldeamlak Bewket & Conway, 2007; Mekonen *et al.*, 2020; Rawashdeh *et al.*, 2024). In addition this result also has similarity with (Yekoy, 2022) which winter, autumn, and summer, along with the entire year, also provided evidence that, apart from the autumn period (2.41 mm per season), the remaing periods exhibited declining pattern within the research area.

The study area, as indicated by the findings, rainfall summer period (June, July and Augest) accounted for most of the total yearly rainfall. Outlined table 1, June contributed 12.8%, July contributed 14.7%, and August contributed 21.05% of the overall rainfall (Feke *et al.*, 2021). The period from 1981 to 2022 witnessed the minimum mean rainfall during the month of December, January and feburuary the dry or winter season the majourity part of Ethiopia encompassing the current research area (Enyew & Wassie, 2024). This result strongly inlined with the study done by Feke *et al.* (2021) at Horro Guduru Wollega Zone of Oromia National Regional State.

As shown in Table 2, the yearly PCI during the period from 1981 and 2022 was primarily defined by erratic rainfall distribution (55.4%) of the observation years. Summer season belongs to erratic rainfall distribution (17.4 %) also spring and autumn season shows irregular and (42.3%) of the seasons respectively. Similar results reported by (Feke *et al.*, 2021; A. Alemayehu *et al.*, 2022; Wassie *et al.*, 2022) from Horro Guduru Wollega Zone of Oromia National Regional State, Suha watershed, Upper Blue Nile Basin, Northwest Ethiopia, and western Ethiopia.

Potential influence of rainfall and temperature variability

The observed spatial and temporal variations in rainfall and temperature could have significant impacts on farming methods and crop yields among smallholder farmers. Adequate and timely rainfall in terms of amount and duration during the winter, spring, summer, autumn, and annual seasons is crucial for agricultural activities. However, the inconsistency and variability of rainfall during spring (March, April, May) and Summer (June, July, August) seasons depressing agricultural practices and productions over the three agro-ecological zones. However, the delayed onset of rainfall in February and the early cessation of rainfall in September have been affecting farmers' ability to plant early and on time, as well as hindering the active growth and maturation of various crops. This ultimately affected farming output by introducing instability into the planting schedule. For instance, authors such as (Dinku, 2010; Asfaw *et al.*, 2018) it was observed that in fluctuation in the quantity and duration of precipitation throughout the spring and summer seasons resulted in losses in agriculture and cattle production, pushing families into persistent food insecurity. Regassa *et al.* (2010) further suggested that spring rainfall may affect the production of long-cycle crops, leading to severe consequences for agricultural output. Similarly, (Bewket, 2009) further predicted that fluctuating rainfall costs 38% of the nation's possible growth rate and rise poverty level by 25%, added that sever rainfall fluctuation is a key driver of fluctuations in cereal growth, leaving subsistence cultivators highly vulnerable to hunger crisis. Additionally, rising pattern in yearly and periodical temperatures during research time could exert significant pressure on the crop production process for smallholder farmers.

The incremental trend yearly and period temperatures when the research time could have a profound effect crop production procedures of family's cultivators. For example, (Daninga *et al.*, 2015) stated that warming will amplify the impact of droughts, which reduces the soil's moisture levels impacting the productivity of agricultural land. (Gebreegziabher *et al.*, 2020) it was also projected that rising annual and seasonal temperatures would reduce crop yields per hectare.

In general, the possible effect of climate fluctuation on agricultural output primarily driven by its sensitivity to changes in pricipitation and temperature. This is because agriculture output has a narrow range of optimal and tolerable rainfall and temperature conditions for healthy growt (Gebreegziabher *et al.*, 2020). In summary, discussions highlight that temperature and precipitation fluctuation significantly reduces agricultural output and undermines the overall success of the agricultural sector. During periods of severe climate variability, these impacts can escalate to complete crop failure, resulting in famine and the loss both human and animal lives (Mekonen *et al.*, 2020).

4. Conclusion

The study identified both temporal and geographical fluctuations in rainfall and temperature in the Jabitehinan district. There were seasonal differences in rainfall trends, with minor increases observed across all seasons and the annual average. Temperature exhibited a consistent increasing trend across all seasons and in annual averages. These findings suggest that the Jabitehinan district is experiencing climate variability, which could impact agriculture, water resources, and ecosystems in this predominantly agrarian region. Rising temperatures may exacerbate evapotranspiration and reduce water availability, while changing rainfall patterns could affect crop productivity. Rainfall distribution showed variability across the district, with higher rainfall in the upper highlands and less in the middle and lower regions. The highest rainfall concentrations were limited to specific parts of the district, highlighting localized disparities. Spatial variations in rainfall could lead to unequal access to water resources, affecting both farming practices and water management. Areas with less rainfall might face greater water stress, requiring adaptive interventions. The decadal increase in temperature across all seasons indicates a long-term warming trend. Long-term warming may intensify climate challenges, such as reduced crop yields, shifts in growing seasons, and increased risks of heat stress for humans and livestock.

This study faced limited temporal coverage of data, if the dataset used for analysis only spans four decades, it may not capture long-term climate variability or extreme events comprehensively. Regional Specificity was another shortcoming of this study; the findings are specific to the Jabitehinan district and may not generalize to other regions of Ethiopia, even those in similar highland environments. The researchers strongly recommended that other scholars include longer datasets and integrate global climate models to validate and predict future trends.

Authors' contributions

1. Addisu Bitew: The main researcher has written the manuscript, collect the data, and conducted the analysis

2. Daniel Ayalew: The second main researcher, has reviewed the paper, grammar and helped write it, and supervised the manuscript. The authors read and approved the final manuscript.

Competing interests

On behalf of all authors, the corresponding author states that there is no conflict of interest.

Funding: - No funding was supported for this research.

Reference

Abegaz, W. B., & Mekoya, A. J. R. (2020). Rainfall variability and trends over Central Ethiopia. Environmental Systems Research, 9(1), 1–13. https://doi.org/10.1186/s40068-020-00175-4

Abtew, W., Melesse, A. M., & Dessalegne, T. (2009). Spatial, inter and intra-annual variability of the Upper Blue Nile Basin rainfall. Hydrological Processes, 23(21), 3075–3082. https://doi.org/10.1002/hyp.7419

Ademe, D., Zaitchik, B. F., Tesfaye, K., Simane, B., Alemayehu, G., & Adgo, E. (2020). Climate trends and variability at adaptation scale: Patterns and perceptions in an agricultural region of the Ethiopian Highlands. Weather and Climate Extremes, 29, 100263. https://doi.org/10.1016/j.wace.2020.100263

Ahmed, S. I., Rudra, R., Dickinson, T., & Ahmed, M. (2014). Trend and periodicity of temperature time series in Ontario. American Journal of Climate Change, 3(3), 272–288. https://doi.org/10.4236/ajcc.2014.33026

Ahrens, B. (2006). Distance in spatial interpolation of daily rain gauge data. Hydrology and Earth System Sciences, 10(2), 197–208. https://doi.org/10.5194/hess-10-197-2006

Alam, G. M. M., Alam, K., & Mushtaq, S. (2017). Climate change perceptions and local adaptation strategies of hazard-prone rural households in Bangladesh. Climate Risk Management, 17, 52–63. https://doi.org/10.1016/j.crm.2017.06.006

Alemayehu, A., Maru, M., Bewket, W., & Assen, M. (2020). Spatiotemporal variability and trends in rainfall and temperature in Alwero watershed, western Ethiopia. Environmental Systems Research, 9(1), 22. https://doi.org/10.1186/s40068-020-00184-3

Alemayehu, Z. Y., Minale, A. S., & Legesse, S. A. (2022). Spatiotemporal rainfall and temperature variability in Suha watershed, Upper Blue Nile Basin, Northwest Ethiopia. Environmental Monitoring and Assessment, 194(8), 538. https://doi.org/10.1007/s10661-022-10165-x

Alemu, Y. T. (2019). Watershed-based rainfall variability and trends of extreme rainfall events in South East Awash Basin, Ethiopia. International Journal of Social Sciences and Humanities Invention, 6(6), 5524–5530. https://doi.org/10.18535/ijsshi/v6i6.07

Asfaw, A., Simane, B., Hassen, A., & Bantider, A. (2018). Variability and time series trend analysis of rainfall and temperature in northcentral Ethiopia: A case study in Woleka sub-basin. Weather and Climate Extremes, 19, 29–41. https://doi.org/10.1016/j.wace.2017.12.002

Ayalew, D., Tesfaye, K., Mamo, G., Yitaferu, B., & Bayu, W. (2012). Variability of rainfall and its current trend in Amhara region, Ethiopia. African Journal of Agricultural Research, 7(10), 1475–1486. https://doi.org/10.5897/AJAR11.698

Bahiru, W., Wende, E., Mohammed, L., Mohammed, Y., Adem, H., & Demmisie, Y. (2020). Assessing the impact of rainfall variability on teff production and farmers' perception at Gubalafto district, North Eastern, Ethiopia. International Journal of Earth Science and Geophysics, 6(2), Article 042. https://doi.org/10.35840/2631-5033/1842

Bewket, W. (2009). Rainfall variability and crop production in Ethiopia: Case study in the Amhara region. In S. Ege, H. Aspen, B. Teferra, & S. Bekele (Eds.), Proceedings of the 16th International Conference of Ethiopian Studies (Vol. 3, pp. 823–836). Norwegian University of Science and Technology. Retrieved from https://www.researchgate.net/publication/265159708

Bewket, W., & Conway, D. (2007). A note on the temporal and spatial variability of rainfall in the drought-prone Amhara region of Ethiopia. International Journal of Climatology, 27(11), 1467–1477. https://doi.org/10.1002/joc.1481

Blein, R., Bwalya, M., Chimatiro, S., Faivre-Dupaigre, B., Kisira, S., Leturque, H., & Wambo-Yamdjeu, A. (2013). Agriculture in Africa: Transformation and outlook. New Partnership for Africa's Development (NEPAD). https://www.researchgate.net/publication/265159708

Cetin, M. (2015). Determining the bioclimatic comfort in Kastamonu City. Environmental Monitoring and Assessment, 187(10), 640. https://doi.org/10.1007/s10661-015-4861-3

Chakraborty, S., Pandey, R. P., Chaube, U. C., & Mishra, S. K. (2013). Trend and variability analysis of rainfall series at Seonath River Basin, Chhattisgarh (India). International Journal of Applied Science and Engineering Research, 2(4), 425–434. https://doi.org/10.6088/ijaser.020400005

Chattopadhyay, S., & Edwards, D. R. (2016). Long-term trend analysis of precipitation and air temperature for Kentucky, United States. Climate, 4(1), Article 10. https://doi.org/10.3390/cli4010010

Daninga, P. D., Mlowosa, T., & Zhao, S. (2015). Farmers' perception and adaptation strategies to climate change indicators in Morogoro. International Journal of Agricultural Sciences and Veterinary Medicine, 3(1), 1–13. https://doi.org/10.6088/ijagvm.2015030101

Degefu, M. A., & Bewket, W. (2014). Variability and trends in rainfall amount and extreme event indices in the Omo-Ghibe River Basin, Ethiopia. Regional Environmental Change, 14(2), 799–810. https://doi.org/10.1007/s10113-013-0538-z

Dinku, T. (2011). Climate risk management and data needs for agriculture in Ethiopia. In Strengthening capacity for climate change adaptation in the agriculture sector in Ethiopia: Proceedings from the national workshop held in Nazareth, Ethiopia, 5–6 July 2010 (pp. 9–14). Food and Agriculture Organization of the United Nations. https://www.fao.org/4/i2155e/i2155e00.pdf

District Agriculture Office. (2020). Annual report for the district agricultural production and other sector implementation. ISSN: 0378-1127. Ethiopian Journal of Agricultural Sciences

Easterling, W. E., Aggarwal, P. K., Batima, P., Brander, K. M., Erda, L., Howden, S. M., Kirilenko, A., Morton, J., Soussana, J.-F., Schmidhuber, J., & Tubiello, F. N. (2007). Food, fibre and forest products. In M. L. Parry, O. F. Canziani, J. P. Palutikof, P. J. van der Linden, & C. E. Hanson (Eds.), Climate change 2007: Impacts, adaptation and vulnerability. Contribution of Working Group II to the Fourth Assessment Report of the Intergovernmental Panel on Climate Change (pp. 273–313). Cambridge University Press.

Enyew, F. B., & Wassie, S. B. (2024). Rainfall trends and spatiotemporal patterns of meteorological drought in Menna watershed, northwestern Ethiopia. Heliyon, 10(6), e27919. https://doi.org/10.1016/j.heliyon.2024.e27919

Esayas, B., Simane, B., Teferi, E., Ongoma, V., & Tefera, N. (2019). Climate variability and farmers' perception in Southern Ethiopia. Advances in Meteorology, 2019, Article 7341465. https://doi.org/10.1155/2019/7341465

Feke, B. E., Terefe, T., Ture, K., & Hunde, D. (2021). Spatiotemporal variability and time series trends of rainfall over northwestern parts of Ethiopia: The case of Horro Guduru Wollega Zone. Environmental Monitoring and Assessment, 193(6), 367. https://doi.org/10.1007/s10661-021-09141-8

Gautam, R., Hsu, N. C., Lau, K.-M., Tsay, S.-C., & Kafatos, M. (2009). Enhanced pre-monsoon warming over the Himalayan-Gangetic region from 1979 to 2007. Geophysical Research Letters, 36(7), L07704. https://doi.org/10.1029/2009GL037641

Gebreegziabher, Z., Mekonnen, A., Bekele, R. D., Zewdie, S. A., & Kassahun, M. M. (2013). Crop-livestock inter-linkages and climate change implications for Ethiopia's agriculture: A Ricardian approach. Resources for the Future Discussion Paper Series, EfD DP 13-14. https://www.rff.org/publications/working-papers/crop-livestock-inter-linkages-and-climate-change-implications-for-ethiopias-agriculture-a-ricardian-approach/

Gebrehiwot, T., van der Veen, A., & Maathuis, B. (2011). Spatial and temporal assessment of drought in the Northern highlands of Ethiopia. International Journal of Applied Earth Observation and Geoinformation, 13(3), 309–321. https://doi.org/10.1016/j.jag.2010.12.002

Gissila, T., Black, E., Grimes, D. I. F., & Slingo, J. M. (2004). Seasonal forecasting of the Ethiopian summer rains. International Journal of Climatology, 24(11), 1345–1358. https://doi.org/10.1002/joc.1078

Hare, W. (2003). Assessment of knowledge on impacts of climate change—Contribution to the specification of Article 2 of the UNFCCC: Impacts on ecosystems, food production, water, and socio-economic systems. Wissenschaftlicher Beirat der Bundesregierung Globale Umweltveränderungen (WBGU). https://www.wbgu.de/wbgu_sn2003_ex01.pdf

Intergovernmental Panel on Climate Change. (2000). Land use, land-use change, and forestry: A special report of the Intergovernmental Panel on Climate Change. Cambridge University Press. https://www.ipcc.ch/report/land-use-land-use-change-and-forestry/

Intergovernmental Panel on Climate Change. (2014). Summary for policymakers. In Climate Change 2014: Impacts, Adaptation, and Vulnerability. Part A: Global and Sectoral Aspects. Contribution of Working Group II to the Fifth Assessment Report of the Intergovernmental Panel on Climate Change. Cambridge University Press. https://www.ipcc.ch/site/assets/uploads/2018/02/WGIIAR5-SPM_Approved.pdf

Jain, S. K., & Kumar, V. (2012). Trend analysis of rainfall and temperature data for India. Current Science, 102(1), 37–49.

Jury, M. R., & Funk, C. (2013). Climatic trends over Ethiopia: Regional signals and drivers. International Journal of Climatology, 33(8), 1924–1935. https://doi.org/10.1002/joc.3560

Khatri, B. B., & Pasa, R. B. (2023). People's perception on climate change: The context of local and global discourse. Asian Journal of Population Sciences, 2(1), 68–79. https://doi.org/10.3126/ajps.v2i1.51091

McSweeney, C., New, M., & Lizcano, G. (2008). UNDP Climate Change Country Profiles: Ethiopia. United Nations Development Programme. https://digital.library.unt.edu/ark:/67531/metadc226682/

Mekonen, A. A., & Berlie, A. B. (2020). Spatiotemporal variability and trends of rainfall and temperature in the Northeastern Highlands of Ethiopia. Modeling Earth Systems and Environment, 6(1), 285–300. https://doi.org/10.1007/s40808-019-00678-9

National Meteorological Services Agency (NMSA). (2007). Climate Change National Adaptation Programme of Action (NAPA) of Ethiopia. NMSA. https://unfccc.int/resource/docs/napa/eth01.pdf

Ndaruzaniye, V. (2011). Water security in Ethiopia: Risks and vulnerabilities assessment. Global Water Institute for Africa Climate Change, Environment and Security. https://gwiwater.org

Philip, S., Kew, S. F., van Oldenborgh, G. J., Otto, F., O'Keefe, S., Haustein, K., King, A., Zegeye, A., Eshetu, Z., Hailemariam, K., Singh, R., Jjemba, E., Funk, C., & Cullen, H. (2018). Attribution analysis of the Ethiopian drought of 2015. Journal of Climate, 31(6), 2465–2486. https://doi.org/10.1175/JCLI-D-17-0274.1

Rawashdeh, S., Thneibat, A. A., Aladwan, Z., Taran, A., & Alrababah, A. (2024). Climate changes on the amount of rain and temperature from 1990–2018 in Madaba, Jordan using geographical information systems. Indonesian Journal of Geography, 56(1), 1–13. https://doi.org/10.22146/ijg.88016

Regassa, S., Givey, C., & Castillo, G. (2010). The rain doesn't come on time anymore: Poverty, vulnerability, and climate variability in Ethiopia. Oxfam International. https://policy-practice.oxfam.org/resources/the-rain-doesnt-come-on-time-anymore-poverty-vulnerability-and-climate-variabil-112339/

Riddle, E. E., & Cook, K. H. (2008). Abrupt rainfall transitions over the Greater Horn of Africa: Observations and regional model simulations. Journal of Geophysical Research: Atmospheres, 113(D15), D15109. https://doi.org/10.1029/2007JD009202

Rosell, S. (2014). Rainfall variability, soils and land use changes in the Ethiopian highlands (Doctoral thesis, University of Gothenburg). Department of Earth Sciences. https://gupea.ub.gu.se/handle/2077/33656

Seleshi, Y., & Zanke, U. (2004). Recent changes in rainfall and rainy days in Ethiopia. International Journal of Climatology, 24(8), 973–983. https://doi.org/10.1002/joc.1052

Sen, P. K. (1968). Estimates of the regression coefficient based on Kendall's tau. Journal of the American Statistical Association, 63(324), 1379–1389. https://doi.org/10.1080/01621459.1968.10480934

Sharma, Y., Sajjad, H., Saha, T. K., Bhuyan, N., Sharma, A., & Ahmed, R. (2024). Analyzing and forecasting climate variability in Nainital district, India using non-parametric methods and ensemble machine learning algorithms. Theoretical and Applied Climatology, 155(6), 4749–4761. https://doi.org/10.1007/s00704-024-04920-

Suryabhagavan, K. V. (2017). GIS-based climate variability and drought characterization in Ethiopia over three decades. Weather and Climate Extremes, 15, 11–23. https://doi.org/10.1016/j.wace.2016.11.005

Tessema, I., & Simane, B. (2019). Vulnerability analysis of smallholder farmers to climate variability and change: An agro-ecological system-based approach in the Fincha'a sub-basin of the upper Blue Nile Basin of Ethiopia. Ecological Processes, 8(1), Article 5. https://doi.org/10.1186/s13717-019-0159-7

Tessema, Y. A., Aweke, C. S., & Endris, G. S. (2013). Understanding the process of adaptation to climate change by small-holder farmers: The case of East Hararghe Zone, Ethiopia. Agricultural and Food Economics, 1(1), Article 13. https://doi.org/10.1186/2193-7532-1-13

Teyso, T., & Anjulo, A. (2016). Spatio-temporal variability and trends of rainfall and temperature over Gamo Gofa Zone, Ethiopia. Journal of Scientific Research and Reports, 12(2), 1–11. https://doi.org/10.9734/JSRR/2016/28667

UNDP. (2007). Population Division of the Department of Economic and Social Affairs of the United Nations Secretariat, world population prospects: The 2006 revision and world urbanization prospects, 2005 revision. United Nations. http://esa.un.org/unpp

UNFCCC. (2007). Climate change: Impacts, vulnerabilities and adaptation in the developing countries. UNFCCC Secretariat. https://unfccc.int/resource/docs/publications/impacts.pdf

UNFCCC. (2015). Measurements for estimation of carbon stocks in afforestation and reforestation project activities under the Clean Development Mechanism: A field manual. United Nations Framework Convention on Climate Change. https://unfccc.int/resource/docs/publications/2015_measurements_cdm.pdf

Wagesho, N., Goel, N. K., & Jain, M. K. (2013). Temporal and spatial variability of annual and seasonal rainfall over Ethiopia. Hydrological Sciences Journal, 58(2), 354–373. https://doi.org/10.1080/02626667.2012.754543

Wassie, S. B., Mengistu, D. A., & Berlie, A. B. (2022). Trends and spatiotemporal patterns of meteorological drought incidence in North Wollo, northeastern highlands of Ethiopia. Arabian Journal of Geosciences, 15(12), Article 1158. https://doi.org/10.1007/s12517-022-10423-9

Yekoy, Z. (2022). Spatiotemporal rainfall and temperature variability in Suha watershed, Upper Blue Nile Basin, Northwest Ethiopia. Environmental Monitoring and Assessment, 194(8), Article 538. https://doi.org/10.1007/s10661-022-10165-x